Identification of Multiple Isolated Lymphoid Follicles on the Antimesenteric Wall of the Mouse Small Intestine[1]

Hiromasa Hamada,*† Takachika Hiroi,‡ Yasuhiro Nishiyama,*§ Hidemi Takahashi,§ Yohei Masunaga,¶ Satoshi Hachimura,¶ Shuichi Kaminogawa,¶ Hiromi Takahashi-Iwanaga,‖ Toshihiko Iwanaga,# Hiroshi Kiyono,‡ Hiroshi Yamamoto,† and Hiromichi Ishikawa*[2]

We have revealed that 100–200 clusters, filled with closely packed lymphocytes, can be found throughout the length of the antimesenteric wall of the mouse small intestine. They are composed of a large B cell area, including a germinal center, and epithelia overlying the clusters contain M cells. A large fraction of B cells displays $B220^+CD19^+CD23^+IgM^{low}IgD^{high}CD5^-Mac\text{-}1^-$ phenotype, and the composition of IgA^+ B cells is smaller but substantial. To our knowledge, these clusters are the first identification of isolated lymphoid follicles (ILF) in mouse small intestine. ILF can be first detected at 7 (BALB/c mice) and 25 (C57BL/6 mice) days after birth, and lymphoid clusters equivalent in terms of cellular mass to ILF are present in germfree, athymic nude, *RAG-2*$^{-/-}$, TCR-$\beta^{-/-}$, and Ig μ-chain mutant ($\mu m^{-/-}$) mice, although c-*kit*$^+$ cells outnumber $B220^+$ cells in germfree and athymic nude mice, and most lymphoid residents are c-*kit*$^+B220^-$ in *RAG-2*$^{-/-}$, TCR-$\beta^{-/-}$, and $\mu m^{-/-}$ mice. ILF develop normally in the progeny of transplacentally manipulated Peyer's patch (PP)-deficient mice, and decreased numbers of conspicuously atrophied ILF are present in IL-7R$\alpha^{-/-}$ PP^{null} mice. Neither ILF nor PP are detectable in lymphotoxin $\alpha^{-/-}$ and *aly/aly* mice that retain well-developed cryptopatches (CP) and thymus-independent subsets of intraepithelial T cells, whereas ILF, PP, CP, and thymus-independent subsets of intraepithelial T cells disappear from common cytokine receptor γ-chain mutant mice. These findings indicate that ILF, PP, and CP constitute three distinct organized gut-associated lymphoid tissues that reside in the lamina propria of the mouse small intestine. *The Journal of Immunology,* **2002, 168: 57–64.**

In the small intestine of mammals, gut-associated lymphoid tissues (GALT)[3] consist of organized lymphoid structures and diffusely distributed populations of cells. Organized GALT are principally comprised of aggregated lymphoid follicles (Peyer's patches; PP) and mesenteric lymph nodes (MLN).

It is now clear that IgA is one of the key hallmarks of the intestinal humoral immune system (1–3) and that PP are the major inductive sites for initiation of Ag-specific IgA responses to a variety of intestinal luminal Ags (4, 5). However, it has been reported that PP are not of paramount importance for establishing strong local IgA Ab responses to foreign protein Ag in rats (6) and to live locally invasive bacteria in rabbit (7). Consistent with these earlier observations, we (8) have recently demonstrated that PP also are not a strict requirement in mice for induction of Ag-specific intestinal IgA Ab responses. Oral immunization of the progeny of mice treated with lymphotoxin β receptor (LTβR) and Ig chimeric protein (LTβR-Ig) that lacked PP but retained MLN (9) with OVA plus cholera toxin as mucosal adjuvant resulted in OVA-specific intestinal IgA Ab responses (8). In contrast, TNF and lymphotoxin (LT) α double-knockout mice that lacked both PP and MLN (10) failed to elicit the responses (8). On the basis of these findings, we underscored the compensatory role of MLN for the induction of mucosal immune responses in LTβR-Ig-treated PP^{null} mice.

Other forms of lymphoid aggregations that have been identified in the wall of human (11), rabbit (7), and guinea pig (12) small intestines are isolated lymphoid follicles (ILF) which are invisible from the serosal or mucosal surface of the small intestine. ILF are structurally and functionally similar to the follicular units that compose PP and are believed to be an equivalent or complementary system to PP for the induction of intestinal IgA Ab responses. In contrast to ILF identified in the above mammals, however, ILF in the mouse small intestine have not been described in the immunological literature to date. Recently, we revealed multiple tiny clusters filled with c-*kit*$^+$IL-7R$^+$Thy-1$^+$ lymphohemopoietic progenitors in crypt lamina propria (LP) of the mouse small intestine (cryptopatches; CP) (13–16) and verified that CP were extrathymic anatomical sites indispensable for intestinal T lymphopoiesis (14–16). The modified nonclassical villi occupied mostly by immature lymphocytes (lymphocyte-filled villi; LFV) have also been identified in the rat small intestine and are regarded as candidates for specialized sites of primary extrathymic T lymphopoiesis (17). In this context, such a continued description of novel GALT is

*Department of Microbiology, Keio University School of Medicine, Tokyo, Japan; †Department of Immunology, Graduate School of Pharmaceutical Science, and ‡Department of Mucosal Immunology, Research Institute for Microbial Diseases, Osaka University, Osaka, Japan; §Department of Microbiology, Nippon Medical School, Tokyo, Japan; ¶Department of Applied Biological Chemistry, University of Tokyo, Tokyo, Japan; ‖Department of Anatomy, School of Medicine, and #Laboratory of Anatomy, Graduate School of Veterinary Medicine, Hokkaido University, Sapporo, Japan

Received for publication August 27, 2001. Accepted for publication October 30, 2001.

The costs of publication of this article were defrayed in part by the payment of page charges. This article must therefore be hereby marked *advertisement* in accordance with 18 U.S.C. Section 1734 solely to indicate this fact.

[1] This work was supported by a Grant-in-Aid for Creative Scientific Research, Ministry of Education, Science, Sports and Culture of Japan; by the Agency of Science and Technology, Japan; by the Japan Society for the Promotion of Science (JSPS-RFTF 97L00701); and by a Keio Gijuku Academic Development Funds.

[2] Address correspondence and reprint requests to Dr. Hiromichi Ishikawa, Department of Microbiology, Keio University School of Medicine, 35 Shinanomachi, Shinjuku-ku, Tokyo 160-8582, Japan. E-mail address: ishikawa@microb.med.keio.ac.jp

[3] Abbreviations used in this paper: GALT, gut-associated lymphoid tissues; *aly*, alymphoplasia; BrdU, bromodeoxyuridine; CP, cryptopatches; CRγ, common cytokine receptor γ-chain; GC, germinal center; GF, germfree; ILF, isolated lymphoid follicles; IEL, intestinal intraepithelial T cells; LFV, lymphocyte-filled villi; LP, lamina propria; LT, lymphotoxin; LTβR, lymphotoxin β receptor; M cells, microfold cells; MLN, mesenteric lymph nodes; μm, Ig μ-chain membrane exon; *nu/nu*, athymic nude; PEC, peritoneal cavity; PI, propidium iodide; PNA, peanut agglutinin; PP, Peyer's patches; *RAG*, recombination-activating gene.

0022-1767/02/$02.00

viewed as a good indication of the complexity of the intestinal immune system that has been driven by millennia of evolutionary pressures (18).

Thus, the continued identification of new organized GALT and a consideration of the reasoning behind this, in conjunction with the significance of our novel findings from LTβR-Ig-treated PP^{null} mice (8), led us to investigate whether lymphoid aggregations equivalent in all respects to ILF are present in the small intestine of laboratory mice. We found that 100–200 lymphoid aggregations that fulfilled the criteria of ILF were aligned along the antimesenteric wall of the mucosa. In the present paper, anatomical structure, organogenesis, lymphocyte composition, and strain-to-strain variation of these newly identified ILF are described in relation to those of the other organized GALT of the mouse small intestine.

Materials and Methods

Mice

BALB/cA/Jcl (B/c), C57BL/6J/Jcl (B6), DBA/2J/Jcl, C3H/HeN/Jcl, athymic nude (*nu/nu*) BALB/cA/Jcl, and alymphoplasia (*aly*) mutant *aly/aly* Jcl (19) mice were purchased from CLEA Japan (Tokyo, Japan). LTα mutant C57BL/6J ($LT\alpha^{-/-}$) mice (20) were purchased from The Jackson Laboratory (Bar Harbor, ME). IL-7R α-chain-deficient ($IL\text{-}7R\alpha^{-/-}$) mice (21), TCR-Cβ mutant ($TCR\text{-}\beta^{-/-}$) mice (22), male mice carrying a truncated mutation of common cytokine receptor γ gene ($CR\gamma^{-/Y}$) (23), and germ-free (GF) BALB/cA mice (24) have been described previously (13, 15). Recombination activating gene-2 mutant ($RAG\text{-}2^{-/-}$) (25) B/c mice were provided by Dr. S. Koyasu (Keio University School of Medicine, Tokyo, Japan). Ig μ-chain membrane exon-deficient ($\mu m^{-/-}$) mice (26) were a generous gift from Dr. H. Karasuyama (Tokyo Medical and Dental University, School of Medicine, Tokyo, Japan). We obtained transplacentally manipulated PP-deficient mice according to the two methods described elsewhere (8, 9, 27). In brief, timed pregnant B/c mice were injected i.v. with 2 mg of an antagonistic mAb to IL-7R (A7R34) on gestational day 14.5 (27) or 200 μg LTβR-Ig chimeric protein on gestational days 14 and 17 (8). All animal procedures described in this study were performed in according with the guidelines for animal experiments of Keio University School of Medicine.

Abs and lectin

The following mAbs described elsewhere (13–16) were used. For immunohistochemical staining: anti-B220 (RA3-6B2; 2 μg/ml), anti-c-*kit* (ACK-2; 5 μg/ml), anti-CD3 (145-2C11; 5 μg/ml), anti-IL-7R (A7R34; 5 μg/ml) and anti-CD11c (N418; supernatant of the cultured hybridoma) mAbs. Biotinylated peanut agglutinin (PNA; 7.5 μg/ml) (Vector Laboratories) was also used in this study. For flow cytometric analysis: 3–15 × 10^5 cells were stained in 50 μl staining medium containing the following mAbs described elsewhere (13–16). FITC-conjugated anti-B220 (RA3-6B2; 5 μg/ml), anti-c-*kit* (ACK-4; 25 μg/ml), and anti-Mac-1 (M1/70; 10 μg/ml) mAbs; and biotinylated anti-IL-7R (A7R34; 30 μg/ml) mAb. FITC-conjugated anti-IgD (11–26c.2a; 20 μg/ml; BD PharMingen, San Diego, CA), anti-IgA (C10-3; 20 μg/ml; BD PharMingen), and anti-T and B cell activation Ag (GL-7; 10 μg/ml; BD PharMingen) mAbs; and biotinylated anti-IgM (R6-60.2; 20 μg/ml, BD PharMingen), anti-B220 (RA3-6B2; 10 μg/ml, BD PharMingen), anti-CD11c (HL3; 10 μg/ml, BD PharMingen), anti-CD5 (53-7.3; 10 μg/ml, BD PharMingen), anti-CD19 (1D3; 10 μg/ml; BD PharMingen), and anti-CD23 (B3B4; 20 μg/ml; BD PharMingen) mAbs as well as biotinylated PNA (0.5 μg/ml; Vector Laboratories) were also used in this study.

Immunohistochemical procedure

Small intestine was longitudinally opened along the mesenteric wall, and then intestine ~10 mm long that had been either kept flat for horizontal section or rolled up for vertical section was embedded in OCT compound (Tissue-Tek; Miles, Elkhalt, IN) at −80°C. The tissue segments were sectioned with a cryostat at 6 μm, and sections were preincubated with Blockace (Dainippon Pharmaceutical, Osaka, Japan) to block nonspecific binding of mAbs. The sections were then incubated with rat or hamster mAb for 30 min at 37°C and rinsed three times with PBS, followed by incubation with biotin-conjugated goat anti-rat IgG Ab (5 μg/ml; Cedarlane Laboratories, Hornby, Ontario, Canada) or with biotin-conjugated goat anti-hamster IgG (5 μg/ml; Cedarlane Laboratories). In staining with biotinylated PNA, the second biotin-conjugated anti-IgG Ab was not used. Subsequently, the sections were washed three times with PBS and then incubated with avidin-biotin peroxidase complexes (Vectastain ABC kit; Vector Laboratories). The histochemical color development was achieved by the Vectastain DAB (3,3′-diaminobenzidine) substrate kit (Vector Laboratories) according to the manufacturer's instructions. Finally, the sections were counterstained with hematoxylin for microscopy. Endogenous peroxidase activity was blocked with 0.3% H_2O_2 and 0.1% NaN_3 in distilled water for 10 min at room temperature. Tissue sections incubated either with isotype-matched normal rat IgG or with nonimmune hamster serum showed only minimal background staining.

In vivo labeling and in situ immunohistochemical visualization of proliferating lymphocytes

Mice were given drinking water containing 1 mg/ml bromodeoxyuridine (BrdU) for 38 h. The small intestines were removed and opened along the mesenteric wall. Then intestines ~10 mm long that had been rolled up were embedded in OCT compound at −80°C. Cryostat tissue sections 9 μm thick that included PP and/or ILF were fixed in 4% paraformaldehyde for 15 min at 4°C, washed three times with PBS, and treated with 2 M HCl for 20 min at 37°C, followed by neutralization with 0.1 M sodium tetraborate. Subsequent immunohistochemical color development using the first anti-BrdU mAb (B44; BD Biosciences, San Jose, CA) and the second biotinylated goat anti-mouse Ig Ab (20 μg/ml; Cappel, Aurora, OH) was performed according to the method described in the preceding section.

Flow cytometry

A single lymphoid cell suspension was prepared, and nucleated cells were counted using a hemocytometer. Resident lymphoid cells in the peritoneal cavity (PEC) were obtained by rinsing PEC with 10 ml ice-cold PBS without Ca^{2+} and Mg^{2+}. ILF cells were isolated by essentially the same technique used for the isolation of CP cells (14–16). In brief, the small intestine was opened longitudinally along the mesenteric wall, and mucus and feces were removed with filter paper. Subsequently, intestine ~10 mm long was pasted on a plastic culture dish. We amputated a needle (18-gauge; inner diameter, 940 μm) at the proximal end of the tapering tip. We then bent the needle in the middle, sharpened its cross-section with the aid of a small electric grinder, i.e., a dental instrument (UA12A; Urawa Kogyo, Saitama, Japan), and finally fitted it on a 1-ml syringe. We located ILF under a transillumination stereomicroscope and isolated a tiny fragment of the small intestine containing one ILF using the needle described above. Lymphoid cells were incubated first with biotinylated mAb and then with streptavidin PE (BD Biosciences) and FITC-conjugated second mAb. Stained cells were suspended in staining medium (Hanks' solution without phenol red, 0.02% NaN_3, and 2% heat-inactivated FBS) containing 0.5 μg/ml propidium iodide (PI) and analyzed using FACScan with CellQuest software (BD Biosciences). Dead cells were excluded by PI gating. Lymphoid cells were incubated with anti-FcγRII/III mAb (2.4G2; 10 μg/ml; BD PharMingen) before staining to block nonspecific binding of labeled mAbs to FcR.

Electron microscopy

Under anesthesia with sodium pentobarbital, B/c mice were perfused transcardially with Ringer's solution and subsequently with a mixture of 2.5% glutaraldehyde and 0.5% paraformaldehyde buffered at pH 7.3 with 0.1 M cacodylate. The small intestine was excised and immersed overnight in the same fixative. After fixation, ILF on the antimesenteric wall were cut out with iridectomy scissors under a dissecting microscope, rinsed in 0.1 M cacodylate buffer (pH 7.3), and postfixed with 1% OsO_4 buffered with cacodylate (0.1 M, pH 7.2) for 2 h. For scanning electron microscopy, the specimens were then dehydrated through a graded series of ethanol, transferred to isoamyl acetate, and critical-point dried with liquid CO_2. The dried specimens were coated with osmium in a plasma osmium coater (Nippon Laser and Electronics Lab, Nagoya, Japan), and examined in a Hitachi H-4500 scanning electron microscope (Hitachi, Tokyo, Japan) at an acceleration voltage of 10 kV. For transmission electron microscopy, the osmicated tissue pieces were dehydrated through a series of ethanol and embedded in Epon 812. Ultrathin sections were examined in a Hitachi H-7100 transmission electron microscope (Hitachi) after double staining with uranyl acetate and lead citrate.

Results

From 100 to 200 lymphoid clusters filled with B220$^+$ cells are distributed throughout the antimesenteric mucosa of the mouse small intestine

During the course of our study on CP (13–16), we noticed the presence of tiny and macroscopically invisible lymphoid clusters filled with B220$^+$ cells in the mouse small intestine, although they are far less frequent but much larger than CP. Recently, we (8) verified that PP are not necessarily obligate GALT for the induction of Ag-specific intestinal IgA and serum IgG Ab responses to an orally administered protein Ag. With these observations in mind, we aimed at investigating the cluster filled with B220$^+$ cells (we use hereafter the term ILF for these B cell aggregations; see below) in detail.

ILF were located in tandem on the antimesenteric wall down from duodenum to ileum in B/c (Fig. 1*A*, *left*) and B6 (data not shown) mice, whereas CP filled with c-*kit*$^+$ cells were interspersed throughout the mucosa (Fig. 1*A*, *middle*). We also confirmed antimesenteric localization of multiple ILF in the small intestines of DBA/2J/Jcl and C3H/HeN/Jcl mice (data not shown). ILF were smaller than B cell-enriched follicular units of PP and lacked interfollicular PP regions that contained mainly T cells (Fig. 1*B*). Absolute numbers of ILF in the small bowels of 8- to 20-wk-old adult B/c and B6 mice were 150–200 and 100–150, respectively, and neonatal intestines from these mice lacked ILF. In B/c mice, ILF were not detected at 4 days after birth but became detectable without exception (preferentially in the duodenal and proximal jejunal mucosa) at the 7th postnatal day, the day when CP were first detected in these mice. Postnatal development of ILF in B/c mice is shown in Fig. 2*A*. We also evaluated the frequency DNA replicating cells in ILF and verified that the net accumulation of BrdU-incorporated DNA-replicating cells in ILF was comparable with that in PP (Fig. 2*B*). We (13) have previously reported that CP can be first detected at 14–17 days after birth in the small intestine of B6 mice. However, ILF in B6 intestine remained unidentifiable until day 25 of postnatal life. Thus, although these observations confirm the difference in the time course of postnatal formation of ILF and CP between B/c and B6 animals, histogenetic events behind this difference remain to be explored.

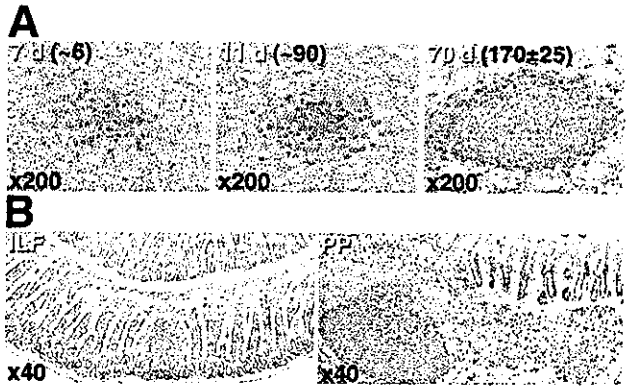

FIGURE 2. Postnatal organogenesis of ILF and immunohistochemical visualization of DNA-replicating cells in ILF. *A*, ILF in B/c mice were not detected at day 4 after birth but became detectable without exception at the 7th postnatal day. The numbers of ILF per small intestine from three to five mice are shown. *B*, BrdU-incorporated lymphocytes in ILF and PP from adult B/c mice. Cells that reside in GC of ILF and PP exhibit massive proliferation.

ILF and CP are distinct organized GALT of the mouse small intestine

CP are located mostly in the crypt LP and are not subdivided into specific areas based on their cellular composition (13). We found in the present study that ILF were larger than CP (Fig. 1*A*) and appeared to occupy both the crypt and villous LP (Fig. 1*B*). To compare more precisely the anatomical and cellular features of ILF with those of CP, immunohistochemical analysis was conducted using five representative mAbs that were reactive with B cells

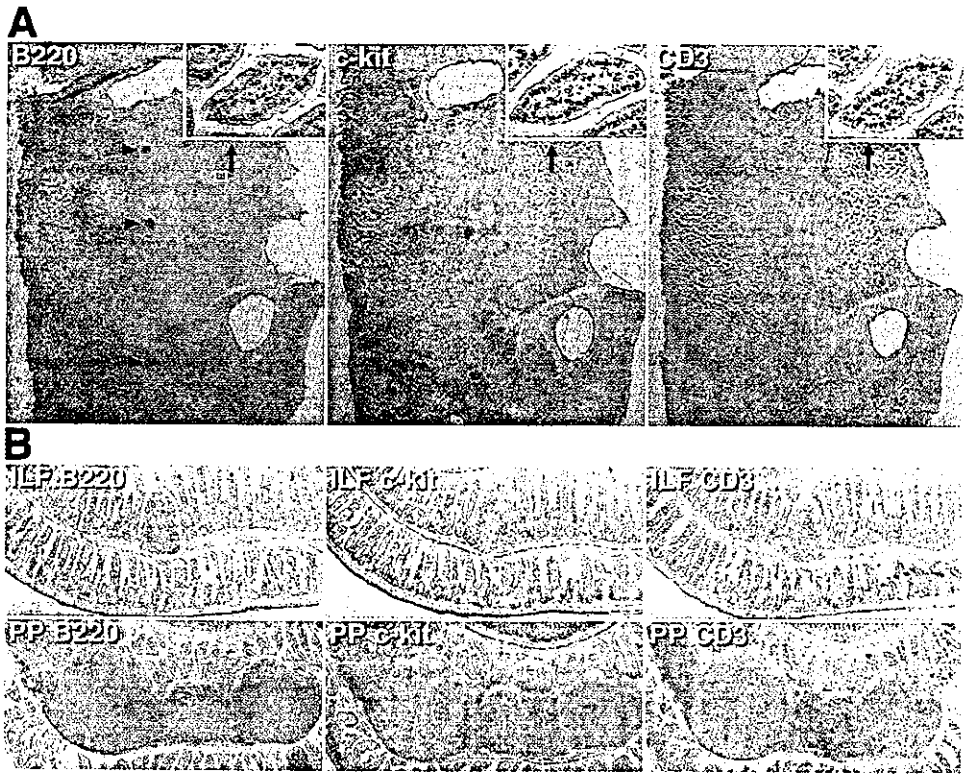

FIGURE 1. Immunohistochemical visualization of B220$^+$ (ILF) and c-*kit*$^+$ (CP) cell aggregations and PP in the small intestine of B/c mice. We examined the entire small intestine, and representative jejunal pictures are shown. *A*, Consecutive tissue sections were stained with anti-B220 (*left*), anti-c-*kit* (*middle*) and anti-CD3 (*right*) mAb, respectively (×15). Three ILF are aligned along the antimesenteric wall of the mucosa (arrowheads) and that numerous tiny CP are interspersed throughout the mucosa. Magnified views (×400) of the rectangular areas are also presented in at the *upper right* (arrows). *B*, Immunohistochemical analysis of ILF and PP on the consecutive vertical tissue sections of the small intestine (×80). Note that ILF lack T (CD3$^+$) cell-enriched interfollicular regions that are the well-acknowledged component of PP (*lower right*).

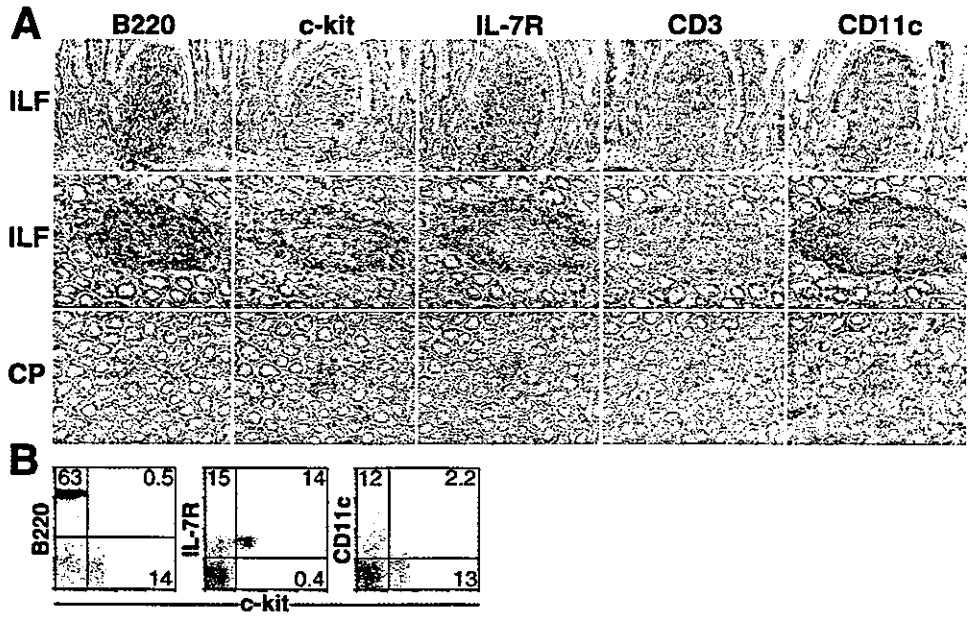

FIGURE 3. Immunohistochemical characterization of cells in ILF and CP and flow cytometric analysis of cells that sojourn in ILF. *A*, Cells expressing B220, c-*kit*, IL-7R, CD3, and CD11c molecules on the consecutive tissue sections were examined by immunohistochemistry (×200). Vertical (*top*) and horizontal (*middle*) profiles of ILF and horizontal (*bottom*) profiles of CP. As also depicted in Fig. 1*B*, villi housing ILF are thicker and shorter in the vertical section than surrounding classical villi and are distinguished by containing LP that are replaced by a major population of cells expressing B220. CP are void of not only $CD3^+$ cells but also $B220^+$ cells. *B*, Two-color flow cytometric analysis of cells isolated from ILF. Note that c-kit^+IL-$7R^+$ cells are neither $B220^+$ nor $CD11c^+$. The percentage of positive cells in the corresponding quadrants is shown.

(B220), mature T cells (CD3), lymphohemopoietic precursor cells (c-kit and IL-7R) or dendritic stromal cells (CD11c), and the results are presented in Fig. 3*A*. On the basis of vertical profile, villi containing ILF were thicker (barrel-shaped) and shorter than surrounding villi not containing ILF (Figs. 1*B* and 3*A*, *top*). The collection of B cells that resided the central region of ILF was surrounded by the layer of cells expressing c-*kit* and IL-7R molecules, and a considerable number of dendritic $CD11c^+$ cells were distributed in the peripheral region of ILF (Fig. 3*A*, *top* and *middle*). Flow cytometric analysis of lymphoid cells isolated from ILF confirmed that the $B220^+$, c-kit^+IL-$7R^+$, and $CD11c^+$ cells constituted three discrete nonoverlapping populations (Fig. 3*B*). A small number of $CD3^+$ T cells was also interspersed within the ILF (Figs. 1*B* and 3*A*). Finally, transverse profiles clearly showed that the average diameter of ILF was longer by a factor of 2–5 compared with that of CP, and, as verified previously (13), neither B cells nor mature T cells were localized in CP (Fig. 3*A*, *bottom*). These findings suggest that ILF and CP constitute two distinct organized GALT in the mouse small intestine.

ILF include germinal center (GC) and epithelia overlying ILF contain microfold (M) cells

During the course of immunohistochemical study on ILF, we realized that the lymphocytes compartmentalized in a core area of the $B220^+$ cell aggregations are proliferating vigorously (Fig. 2*B*) and appear to include B blasts. In lymphoid follicles, B cells at active immune responses can be identified by their distinctive ability to bind PNA (28) and the mAb GL-7 (29, 30) and undergo clonal expansion in forming GC. In this context, we examined whether or not these putative B blasts were capable of binding PNA and found that, in addition to the well-known GC formation in PP (Fig. 4*A*, *bottom*), PNA^+ cell clusters, namely GC, were present in the central area of the $B220^+$ cell aggregations (Fig. 4*A*, *upper left* and *middle*). In contrast, CP were void of such PNA-reactive cells (Fig. 4*A*, *upper right*). Among cells isolated from ILF, PP, MLN, and spleen of nonimmunized normal B/c mice examined, a substantial fraction of $B220^+$ ILF cells was PNA^+ and/or $GL\text{-}7^+$, and a large fraction of $B220^+$ PP cells was PNA^+ and/or $GL\text{-}7^+$, whereas only a minimal fraction of $B220^+$ MLN cells and $B220^+$ splenic cells displayed PNA^+ and/or $GL\text{-}7^+$ phenotypes (Fig. 4*B*), indicating the persistent GC formation in ILF and PP due to the constant antigenic challenge from the gastrointestinal tract.

Follicle-associated epithelium not only has typical columnar enterocytes but also contains M cells that deliver various luminal Ags

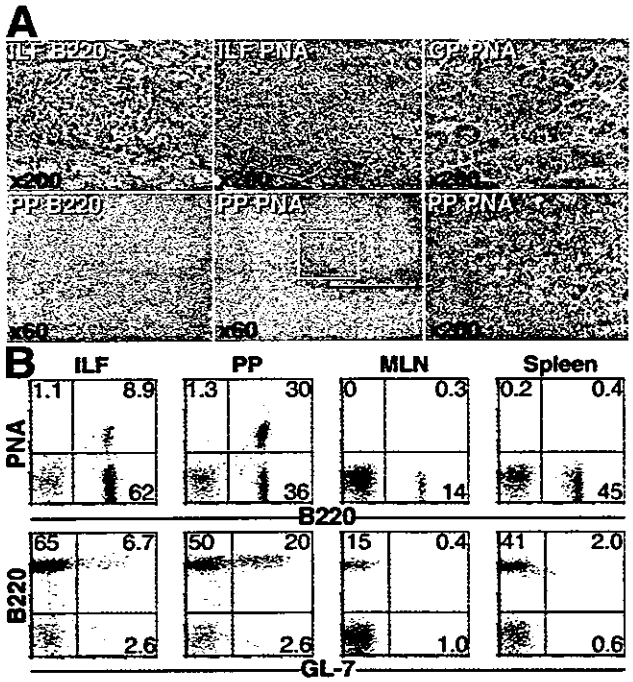

FIGURE 4. Immunohistochemical and flow cytometric verification of GC formation in ILF. *A*, A cluster of PNA binding (PNA^+) cells (*upper middle*) is compartmentalized in the central region of $B220^+$ cell aggregation (*upper left*), namely, ILF, and CP are void of such PNA^+ cells (*upper right*). In the lower panels, one well-established cluster of PNA^+ PP cells (GC) (*middle*) and the surrounding corona of $B220^+$ B cells (*left*) are shown as a positive control. *B*, Two-color flow cytometric analysis was performed on cells isolated from ILF, PP, MLN, and spleen. Although the population size of PNA^+ and/or $GL\text{-}7^+$ subsets of ILF compartment is smaller than that of PP, a significant fraction of cells in ILF expresses ligands for PNA and GL-7, indicating the presence of GC B cells in ILF. In contrast, few if any cells from MLN and spleen are PNA^+ and/or $GL\text{-}7^+$. The percentage of positive cells in the corresponding quadrants is shown.

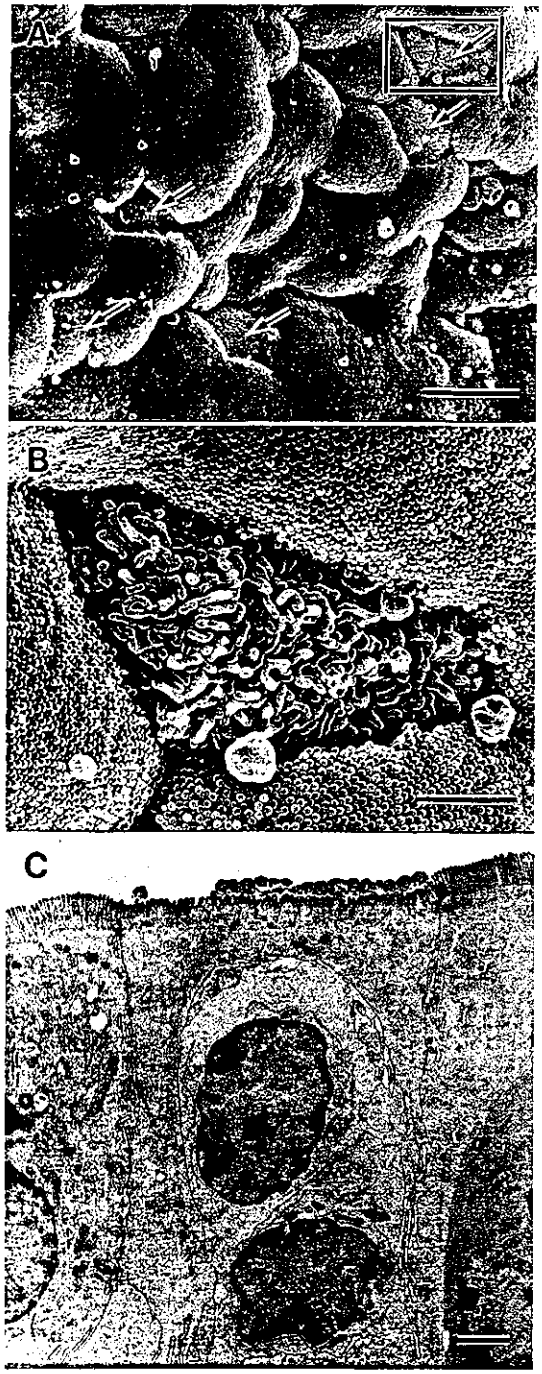

FIGURE 5. Electron microscopic analysis of the epithelium adjacent to ILF. *A*, Scanning electron micrograph of epithelium overlying ILF which shows the presence of five M cells (arrows). Bar, 10 μm. *B*, Magnified view of the *inset* in Fig. 4*A*. The M cell in the center is surrounded by absorptive enterocytes that possess numerous closely packed regular microvilli on their apices. Note the short, wide and irregular microvilli of the M cell. Bar, 2 μm. *C*, Transmission electron micrograph of M cell in the epithelium overlying ILF. Microvilli of the M cell (*center*) are shorter, thicker, and less abundant than those of surrounding absorptive enterocytes, and this M cell enfolds two lymphoid cells. Bar, 2 μm.

to GALT (31). Electron microscopy of epithelia overlying the $B220^+$ cell aggregations revealed that the epithelia contained M cells (Figs. 5, *A* and *B*), and these M cells were found to enfold lymphoid cells in their central hollow (Fig. 5*C*). Thus, taking all of the above findings collectively, these $B220^+$ cell aggregations are the first identification of ILF in the mouse small intestine.

Flow cytometric analysis of B cells that reside in ILF

IgA is a predominant Ig which is secreted mainly across mucous membranes, and the LP of intestines contains the largest collection of IgA-producing plasma cells. These plasma cells have been shown to derive either from the conventional Ag-specific IgA-committed B-2 cells in PP (4, 32) or from the B-1 cells (33, 34) that are enriched among B cells compartmentalized in the PEC (35). To determine whether B cells that reside in ILF are similar or dissimilar to those of PP, flow cytometric analysis was conducted (Fig. 6). Both ILF and PP harbored a large population of IgM^+ B cells and also a significant population of IgA^+ B cells, whereas MLN contained few IgA^+ B cells (Fig. 6, *top*). B cells isolated from ILF, PP, and MLN appeared to be $IgM^{low}IgD^{high}$ as compared with those recovered from PEC, the majority of which displayed $IgM^{high}IgD^{low}$ phenotype (Fig. 6, *middle*). In contrast to the fact that two-thirds of $B220^+$ PEC cells expressed CD5 (Fig. 6, *bottom*) and Mac-1 (data not shown) molecules, such $B220^+CD5^+$ cells (Fig. 6, *bottom*) and $B220^+$Mac-1^+ cells (data not shown) were minimal in ILF, PP, and MLN compartments. Moreover, almost all $B220^+$ cells from ILF and PP were $CD19^+$, and a large fraction of them were $CD23^+$, whereas $B220^+$ cells from PEC remained $CD23^-$ (data not shown). Because mucosal B cells have been classified into B-1 and B-2 cells based on the differential expression of B220, IgM, IgD, CD5, Mac-1, and CD23 molecules (34, 36), the present findings suggest that ILF are inductive sites for initiation of IgA-committed B-2 cell responses in the gastrointestinal tract.

ILF in GF, various mutant and transplacentally manipulated PP-deficient mice

Immunohistochemical analysis was conducted to characterize ILF of GF and various mutant mice (Fig. 7). We evaluated the effects of microbial and thymic deprivations in GF (Fig. 7*B*) and *nu/nu* (Fig. 7*C*) mice, respectively, on the development of ILF and found that the cellularity of ILF remained the same in both animals. However, c-kit^+ cells outnumbered $B220^+$ cells (Fig. 7, *B* and *C*) and the formation of GC was hardly detectable (data not shown) under these conditions. The cellular mass of ILF was also not significantly altered in the *RAG-*$2^{-/-}$ (Fig. 7*D*), TCR-$\beta^{-/-}$ (Fig.

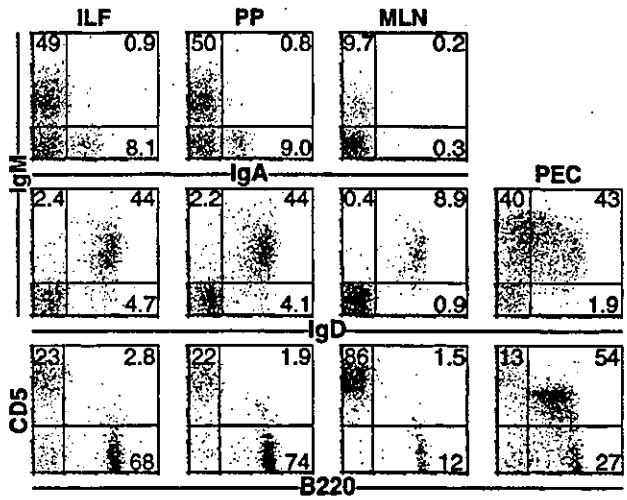

FIGURE 6. B cells that reside in ILF are B-2 rather than B-1 B cells and are phenotypically similar to those that reside in PP but dissimilar to those recovered from PEC, a large fraction of which displays the phenotype of B-1 B cells. Two-color flow cytometric analysis was performed on cells isolated from ILF, PP, MLN, and PEC. The percentage of positive cells in the corresponding quadrants is shown.

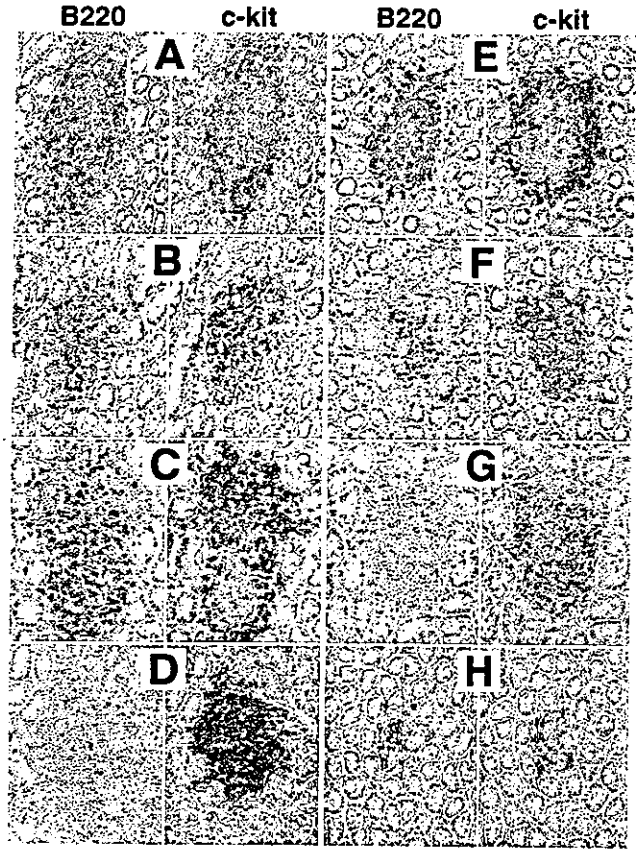

FIGURE 7. Representative immunohistochemical visualization of B220$^+$ and c-*kit*$^+$ lymphocytes in jejunal ILF from wild-type B/c (*A*), GF (*B*), *nu/nu* (*C*), *RAG-2*$^{-/-}$ (*D*), wild-type B6 (*E*), TCR-$\beta^{-/-}$ (*F*), $\mu m^{-/-}$ (*G*) and IL-7R$\alpha^{-/-}$ (*H*) mice. Mice *A–D* have a genetic background of the B/c strain and mice *E–H* have a genetic background of the B6 strain. Original magnification, ×400.

7*F*), and $\mu m^{-/-}$ (Fig. 7*G*) conditions as compared with those of wild-type ILF from B/c (Fig. 7*A*) and B6 (Fig. 7*E*) mice, whereas the difference in cellular composition was striking. Thus, the population size of B220$^+$ cells was reduced drastically in TCR-$\beta^{-/-}$ ILF (Fig. 7*F*), and few, if any, B220$^+$ cells were detected in *RAG-2*$^{-/-}$ (Fig. 7*D*) and $\mu m^{-/-}$ (Fig. 7G) ILF. In these three mutant ILF, especially in *RAG-2*$^{-/-}$ and $\mu m^{-/-}$ ILF, c-*kit*$^+$ cells replaced B220$^+$ cells as the predominant population. As far as the lymphoid residents of PP are concerned, c-*kit*$^+$ cells occupied interfollicular T cell regions in TCR-$\beta^{-/-}$ PP, follicular B cell regions in $\mu m^{-/-}$ PP and entire T and B cell regions in *RAG-2*$^{-/-}$ PP (data not shown). As in the histogenesis of CP (13, 15), sharply emaciated ILF were detected in IL-7R$\alpha^{-/-}$ mice (Fig. 7*H*).

To determine whether ILF are newly identified murine GALT distinct in terms of organogenesis from PP, we determined the number of ILF in various animals, and the results obtained are presented in Table I. Absolute numbers of ILF were not significantly altered in GF, *nu/nu*, *RAG-2*$^{-/-}$, and TCR-$\beta^{-/-}$ mice as compared with those of the corresponding wild-type ILF, whereas absolute numbers of ILF in $\mu m^{-/-}$ mice were about one-half of those in B6 mice. Finally, a drastically reduced number of ILF was detected in IL-7R$\alpha^{-/-}$ PP^{null} mice. It has been reported that PP are absent from the small intestines of LT$\alpha^{-/-}$ (20) and *aly/aly* (19) mutant mice. In this context, we addressed whether these mutations affect the development of ILF and found that histogenesis of ILF was also completely blocked. In these mutant conditions, however, histogenesis of CP and intestinal development of intraepithelial T cells (IEL) that derive from c-*kit*$^+$ CP cells (14, 16) remained intact. It has recently been verified that not only PP but also CP are absent from *CR*$\gamma^{-/-}$ mice. We found that ILF were hardly detectable in the intestinal LP of these *CR*$\gamma^{-/-}$ mice. We also determined the development of ILF in the transplacentally manipulated PP^{null} mice because previous studies have shown that exposure to anti-IL-7R mAb (27) as well as exposure to LTβR-Ig chimeric protein (8, 9) during gestation disrupted PP but not MLN formation. As a result, it was confirmed that the offspring from these mothers lacked PP but possessed well-developed ILF (Table I) and CP (data not shown). In conclusion, ILF are not identical with PP or with CP with respect to their histogenesis and lymphocyte composition, and it is quite intriguing that they are aligned along the antimesenteric wall of the mouse small intestine.

Table I. *Number of ILF and PP in the small intestine of various mice*[a]

	Mice (*n*)	ILF	PP
A.	B/c (11)	178 ± 31	9.0 ± 1.8
	GF (4)	157 ± 15	9.5 ± 1.3[b]
	nu/nu (4)	152 ± 12	8.5 ± 3.1
	RAG-2$^{-/-}$ (4)	129 ± 20	8.5 ± 1.3[c]
	Anti-IL-7R[d] (5)	168 ± 25	UD
	LTβR-Ig[e] (3)	174 ± 16	UD
B.	B6 (6)	143 ± 16	8.0 ± 1.8
	TCR-$\beta^{-/-}$ (4)	134 ± 17	7.8 ± 1.0
	$\mu m^{-/-}$ (4)	70 ± 18	6.5 ± 1.3[b]
	IL-7R$\alpha^{-/-}$ (4)	36 ± 6[c]	UD
	LT$\alpha^{-/-}$ (4)	UD	UD
	aly/aly (5)	UD	UD
	CR$\gamma^{-/-}$ (6)	UD	UD

[a] Immunohistochemical verification of the small intestine in various mice carrying B/c (A) or B6 (B) genetic background. The numbers of ILF and PP per mouse ± SD are presented. UD, undetectable.
[b] Significantly attenuated in size.
[c] Sharply attenuated in size.
[d] Mother B/c mice were injected i.v. with 2 mg anti-IL-7R mAb (A7R34) on gestational day 14.5.
[e] Mother B/c mice were injected i.v. with 200 μg LTβR-Ig chimeric protein on gestational days 14 and 17.

Discussion

To our knowledge, we are the first to identify ~100–200 lymphoid aggregations that satisfied the structural and cellular requirements of ILF in mouse small intestine. Remarkably, they were aligned at roughly regular intervals along the antimesenteric wall of the small bowel (Fig. 1*A*, *left*). In addition to ~10 aggregated lymphoid follicles (37), we also verified that ~50 ILF were interspersed throughout the large intestinal mucosa of B/c mice (data not shown). We do not know why they have not been described to date, but we believe the existence of CP and ILF in the murine intestinal mucosa has not been previously evaluated and reported simply because they are very small and constitute only a thinly scattered population. Immunohistochemical examination revealed that villi housing ILF are thicker and shorter in a longitudinal section than surrounding classical villi, and they are distinguished by containing a LP that is replaced by closely packed lymphocytes (Figs. 1*B* and 3*A*). In this regard, ILF are structures that resemble most closely LFV of the rat small intestine (17), although their lymphoid residents are markedly different from those of rat LFV, a large fraction of which displays an immature phenotype (17). Thus, in agreement with the properties of ILF described in other mammals (7, 11, 12), it is evident that mouse ILF identified in the present study are similar to the follicular units that compose PP.

As far as organogenesis is concerned, however, the difference between ILF and PP is a matter of considerable interest. First, ILF

are not detectable until day 4 (B/c mice) or day 25 (B6 mice) of postnatal life, whereas PP are already microscopically well developed by just before birth in both strains of mouse (Ref. 27 and data not shown). Second, in utero treatment with anti-IL-7R mAb or LTβR-Ig chimeric protein abrogates the development of PP, leaving that of ILF unaffected. Third, IL-7Rα$^{-/-}$ mice lack PP, whereas they possess ILF-like lymphoid aggregations although they are atrophied markedly in both average size (Fig. 7*H*) and numbers. Because the present findings (Figs. 4 and 6) support the notion that ILF are also the inductive sites for intestinal IgA Ab responses to a variety of luminal Ags, the biological significance of the difference in ILF and PP formation is most likely to be failsafe and/or mutually compensatory systems for the maintenance of intestinal immune surveillance. In mice, organogenesis of 6 to 12 PP involves at least 3 distinct steps in the late embryonic stage (27). Exposure of day 14.5 to 15.5 fetuses, namely, the first step, to anti-IL-7R mAb results in the generation of PP^{null} but otherwise normal mice (Ref. 27 and Table I), indicating that there exists a short and critical time window during the initial step of PP formation. In contrast, organogenesis of ILF commences in early postnatal life and thereafter increases gradually in numbers and average size (Fig. 2*A*). In the context of these findings and given that PP have evolved earlier than ILF, it is conceivable that the development of ILF in the mouse small intestine is a failsafe system. Conversely, if the ILF evolved earlier than PP, the development of PP is regarded as a complementary system to the lack of ILF during early infantile life. In any case, exploration of these possibilities is certainly an important goal for future experiments.

Not only PP but also ILF are absent from LTα$^{-/-}$ and *aly/aly* mice, whereas CP and their IEL descendants are present in these mutant animals (14, 16, 38) and, in contrast to antimesenteric distribution of PP and ILF, CP are situated randomly around the circumference of the intestinal wall (Fig. 1*A*). Intriguingly, however, organogeneses of ILF and CP commence at the same postnatal age in B/c mice, although that of PP is completed just before birth. Because it has recently been demonstrated that LTα1β2 receptor (LTβR) signaling is crucial for the first step of PP formation (27) and that LTβR-mediated activation of NF-κB-inducing kinase is selectively cancelled in the *aly* mutation (39), it is evident that the signal passing through LTβR at antimesenteric organizing centers is indispensable for the formation of both PP and ILF anlagen. In sharp contrast, neither LTα1β2 nor the positional signals that emanate solely from antimesenteric mucosa are essential for the formation of CP anlagen. Also, the lymphoid follicles in the cecum (cecal patch), which are surprisingly quite intact in IL-7Rα$^{-/-}$ mice (27), are absent in LTα$^{-/-}$ and *aly/aly* mice (H. Yoshida, unpublished observations). All in all, LTα$^{-/-}$ and *aly/aly* mice lack PP, ILF, and cecal patch but possess well-developed CP, IL-7Rα$^{-/-}$ mice lack PP but possess normal cecal patch and conspicuously atrophied ILF and CP, and *CR*γ$^{-/-}$ mice are void of PP, ILF, and CP. Taking these observations at face value, there exists remarkable complexity in the organogenetic mechanism of different GALT, and much remains to be learned about molecular level of cellular events underlying the formation of these organized GALT before we elucidate the biological significance of this complexity.

In addition to PP and CP, lymphoid aggregations analogous to ILF of wild-type mice are present in *nu/nu*, *RAG-2*$^{-/-}$, and μm$^{-/-}$ mice, indicating that organogenesis of ILF anlagen is dependent neither on thymus-derived lymphocytes nor on the expression of Ag receptor genes on T and B cells. However, ILF detected in *RAG-2*$^{-/-}$ and μm$^{-/-}$ mice are phenotypically abnormal because most lymphoid cells express c-*kit* but not B220 molecules (Figs. 7, *D* and *G*). These results not only indicate that the organogenesis of ILF proceeds through at least several histologically distinct steps but also suggest that B lineage-committed cells and/or mature B cells immigrate from outside into ILF during the latter stage of ILF formation. In conclusion, the current studies identified and characterized ILF in mouse small intestine and illuminated the various facets of their postnatal development. We consider that our findings are of considerable importance because researchers exploring the distinctive features of intestinal immune responses to luminal Ags such as the regulation of mucosal IgA Ab responses and induction of oral tolerance in the gastrointestinal tract, and the role of PP in these processes have been performing their experiments using various manipulated laboratory mice, including the mice that lack PP but possess ILF.

Acknowledgments

We thank Drs. S. Koyasu and H. Karasuyama for providing RAG-2$^{-/-}$ BALB/c mice and μm$^{-/-}$ mice, respectively, and K. Ishimaru and Y. Harashima for their technical assistance.

References

1. Neutra, M. R., P. Michetti, and J.-P. Kraehenbuhl. 1994. Secretory immunoglobulin A: induction, biogenesis, and function. In *Physiology of the Gastrointestinal Tract*, 3rd ed., Vol. 2. L. R. Johnson, ed. Raven Press, New York, p. 685.
2. Russell, M. W., M. Kilian, and M. E. Lamm. 1999. Biological activities of IgA. In *Mucosal Immunology*. 2nd ed. P. L. Ogra, J. Mestecky, M. E. Lamm, W. Strober, J. Bienestock, and J. R. McGhee, eds. Academic Press, San Diego, p. 225.
3. Macpherson, A. J., D. Gatto, E. Sainsbury, G. R. Harriman, H. Hengartner, and R. M. Zinkernagel. 2000. A primitive T cell-independent mechanism of intestinal mucosal IgA responses to commensal bacteria. *Science 288:2222.*
4. Craig, S. W., and J. J. Cebra. 1971. Peyer's patches: an enriched source of precursors for IgA-producing immunocytes in the rabbit. *J. Exp. Med. 134:188.*
5. McIntyre, T. M., and W. Strober. 1999. Gut-associated lymphoid tissue: regulation of IgA B-cell development. In *Mucosal Immunology*. R. L. Ogra, J. Mestecky, M. E. Lamm, W. Strober, J. Bienenstock, and J. R. McGhee, eds. Academic Press, San Diego, p. 319.
6. Heatley, R. V., J. M. Stark, P. Horsewood, E. Bandouvas, F. Cole, and J. Bienenstock. 1981. The effects of surgical removal of Peyer's patches in the rat on systemic antibody responses to intestinal antigen. *Immunology 44:543.*
7. Keren, D. F., P. S. Holt, H. H. Collins, P. Gemski, and S. B. Formal. 1978. The role of Peyer's patches in the local immune response of rabbit ileum to live bacteria. *J. Immunol. 120:1892.*
8. Yamamoto, M., P. Rennert, J. R. McGhee, M.-N. Kweon, S. Yamamoto, T. Dohi, S. Otake, H. Bluethmann, K. Fujihashi, and H. Kiyono. 2000. Alternate mucosal immune system: organized Peyer's patches are not required for IgA responses in the gastrointestinal tract. *J. Immunol. 164:5184.*
9. Rennert, P. D., J. L. Browning, and P. S. Hochman. 1997. Selective disruption of lymphotoxin ligands reveals a novel set of mucosal lymph nodes and unique effects on lymph node cellular organization. *Int. Immunol. 9:1627.*
10. Eugster, H.-P., M. Muller, U. Karrer, B. D. Car, B. Schnyder, V. M. Eng, G. Woerly, M. Le Hir, F. di Padova, M. Aguet, et al. 1996. Multiple immune abnormalities in tumor necrosis factor and lymphotoxin-α double-deficient mice. *Int. Immunol. 8:23.*
11. Moghaddami, M., A. Cummins, and G. Mayrhofer. 1998. Lymphocyte-filled villi: comparison with other lymphoid aggregations in the mucosa of the human small intestine. *Gastroenterology 115:1414.*
12. Rosner, A. J., and D. F. Keren. 1984. Demonstration of M cells in the specialized follicle-associated epithelium overlying isolated lymphoid follicles in the gut. *J. Leukocyte Biol. 35:397.*
13. Kanamori, Y., K. Ishimaru, M. Nanno, K. Maki, K. Ikuta, H. Nariuchi, and H. Ishikawa. 1996. Identification of novel lymphoid tissues in murine intestinal mucosa where clusters of c-*kit*$^+$IL-7R$^+$Thy-1$^+$ lympho-hemopoietic progenitors develop. *J. Exp. Med. 184:1449.*
14. Saito, H., Y. Kanamori, T. Takemori, H. Nariuchi, E. Kubota, H. Takahashi-Iwanaga, T. Iwanaga, and H. Ishikawa. 1998. Generation of intestinal T cells from progenitors residing in gut cryptopatches. *Science 280:275.*
15. Oida, T., K. Suzuki, M. Nanno, Y. Kanamori, H. Saito, E. Kubota, S. Kato, M. Itoh, S. Kaminogawa, and H. Ishikawa. 2000. Role of gut cryptopatches in early extrathymic maturation of intestinal intraepithelial T cells. *J. Immunol. 164:3616.*
16. Suzuki, K., T. Oida, H. Hamada, O. Hitotsumatsu, M. Watanabe, T. Hibi, H. Yamamoto, E. Kubota, S. Kaminogawa, and H. Ishikawa. 2000. Gut cryptopatches: direct evidence of extrathymic anatomical sites for intestinal T lymphopoiesis. *Immunity 13:691.*
17. Mayrhofer, G., M. Moghaddami, and C. Murphy. 1999. Lymphocyte-filled villi (LFV): non-classical organized lymphoid tissues in the mucosa of the small intestine. *Mucosal Immunol. Update 7:9.*
18. Lefrancois, L., and L. Puddington. 1998. Anatomy of T-cell development in the intestine. *Gastroenterology 115:1588.*
19. Miyawaki, S., Y. Nakamura, H. Suzuka, M. Koba, R. Yasumizu, S. Ikehara, and Y. Shibata. 1994. A new mutation, *aly*, that induces a generalized lack of lymph nodes accompanied by immunodeficiency in mice. *Eur. J. Immunol. 24:429.*

20. De Togni, P., J. Goellner, N. H. Ruddle, P. R. Streeter, A. Fick, S. Mariathasan, S. C. Smith, R. Carlson, L. P. Shornick, J. Strauss-Schoenberger, J. H. Russell, R. Karr, and D. D. Chaplin. 1994. Abnormal development of peripheral lymphoid organs in mice deficient in lymphotoxin. *Science 264:703.*
21. Maki, K., S. Sunaga, Y. Komagata, Y. Kodaira, A. Mabuchi, H. Karasuyama, K. Yokomuro, J. Miyazaki, and K. Ikuta. 1996. Interleukin 7 receptor-deficient mice lack γδ T cells. *Proc. Natl. Acad. Sci. USA 93:7172.*
22. Mombaerts, P., A. R. Clarke, M. A. Rudnicki, J. Iacomini, S. Itohara, J. J. Lafaille, L. Wang, Y. Ichikawa, R. Jaenisch, M. L. Hooper, and S. Tonegawa. 1992. Mutations in T-cell antigen receptor genes α and β block thymocyte development at different stages. *Nature 360:225.*
23. Ohbo, K., T. Suda, M. Hashiyama, A. Mantani, M. Ikebe, M. Miyakawa, M. Moriyama, M. Nakamura, M. Katsuki, K. Takahashi, K. Yamamura, and K. Sugamura. 1996. Modulation of hematopoiesis in mice with a truncated mutant of the interleukin-2 receptor γ chain. *Blood 87:956.*
24. Kawaguchi, M., M. Nanno, Y. Umesaki, S. Matsumoto, Y. Okada, Z. Cai, T. Shimamura, Y. Matsuoka, M. Ohwaki, and H. Ishikawa. 1993. Cytolytic activity of intestinal intraepithelial lymphocytes in germ-free mice is strain dependent and determined by T cells expressing γδ T-cell antigen receptors. *Proc. Natl. Acad. Sci. USA 90:8591.*
25. Shinkai, Y., G. Rathbun, K. P. Lam, E. M. Oltz, V. Stewart, M. Mendelsohn, J. Charron, M. Datta, F. Young, A. M. Stall, and F. W. Alt. 1992. RAG-2-deficient mice lack mature lymphocytes owing to inability to initiate V(D)J rearrangement. *Cell 68:855.*
26. Kitamura, D., J. Roes, R. Kuhn, and K. Rajewsky. 1991. A B cell-deficient mouse by targeted disruption of the membrane exon of the immunoglobulin μ chain gene. *Nature 350:423.*
27. Yoshida, H., K. Honda, R. Shinkura, S. Adachi, S. Nishikawa, K. Maki, K. Ikuta, and S.-I. Nishikawa. 1999. IL-7 receptor α^+ $CD3^-$ cells in the embryonic intestine induces the organizing center of Peyer's patches. *Int. Immunol. 11:643.*
28. Rose, M. L., M. S. C. Birbeck, V. J. Wallis, J. A. Forrester, and A. J. S. Davies. 1980. Peanut lectin binding properties of germinal centres of mouse lymphoid tissue. *Nature 284:364.*
29. Han, S., B. Zheng, D. G. Schatz, E. Spanopoulou, and G. Kelsoe. 1996. Neoteny in lymphocytes: Rag1 and Rag2 expression in germinal center B cells. *Science 274:2094.*
30. Laky, K., L. Lefrancois, E. G. Lingenheld, H. Ishikawa, J. M. Lewis, S. Olson, K. Suzuki, R. E. Tigelaar, and L. Puddington. 2000. Enterocyte expression of IL-7 induces development of γδ T cells and Peyer's patches. *J. Exp. Med. 191: 1569.*
31. Owen, R. L. 1999. Uptake and transport of intestinal macromolecules and microorganisms by M cells in Peyer's patches—a personal and historical perspective. *Semin. Immunol. 11:157.*
32. Husband, A. J., and J. L. Gowans. 1978. The origin and antigen-dependent distribution of IgA-containing cells in the intestine. *J. Exp. Med. 148:1146.*
33. Hayakawa, K., R. R. Hardy, D. R. Parks, and L. A. Herzenberg. 1983. The "Ly-1 B" cell subpopulation in normal immunodefective, and autoimmune mice. *J. Exp. Med. 157:202.*
34. Fagarasan, S., and T. Honjo. 2000. T-independent immune response: New aspects of B cell biology. *Science 290:89.*
35. Kroese, F. G. M., E. C. Butcher, A. M. Stall, P. A. Lalor, S. Adams, and L. A. Herzenberg. 1989. Many of the IgA producing plasma cells in murine gut are derived from self-replenishing precursors in the peritoneal cavity. *Int. Immunol. 1:75.*
36. Hardy, R. R., and K. Hayakawa. 1994. CD5 B cells, a fetal B cell lineage. *Adv. Immunol. 55:297.*
37. Owen, R. L., A. J. Piazza, and T. H. Ermak. 1991. Ultrastructural and cytoarchitectural features of lymphoreticular organs in the colon and rectum of adult BALB/c mice. *Am. J. Anat. 190:10.*
38. Nanno, M., S. Matsumoto, R. Koike, M. Miyasaka, M. Kawaguchi, T. Masuda, S. Miyawaki, Z. Cai, T. Shimamura, Y. Fujiura, and H. Ishikawa. 1994. Development of intestinal intraepithelial T lymphocytes is independent of Peyer's patches and lymph nodes in *aly* mutant mice. *J. Immunol. 153:2014.*
39. Shinkura, R., K. Kitada, F. Matsuda, K. Tashiro, K. Ikuta, M. Suzuki, K. Kogishi, T. Serikawa, and T. Honjo. 1999. Alymphoplasia is caused by a point mutation in the mouse gene encoding NF-κB-inducing kinase. *Nat. Genet. 22:74.*

Clinical Immunology
Vol. 102, No. 3, March, pp. 237–248, 2002
doi:10.1006/clim.2001.5166, available online at http://www.idealibrary.com on IDEAL®

Colitis-Related Public T Cells Are Selected in the Colonic Lamina Propria of IL-10-Deficient Mice

Ichiro Takahashi,* Jennifer Matsuda,† Laurent Gapin,† Hilde DeWinter,† Yasuyuki Kai,* Hiroshi Tamagawa,* Mitchell Kronenberg,† and Hiroshi Kiyono*

Department of Mucosal Immunology, Research Institute for Microbial Diseases, Osaka University, 3-1 Yamadaoka, Suita-Osaka 565-0871, Japan; and †Division of Developmental Immunology, The La Jolla Institute for Allergy and Immunology, 10355 Science Center Drive, San Diego, California 92121

IL-10 is an important regulatory cytokine in the mucosal immune system, as supported by the fact that mice deficient in IL-10 spontaneously develop Crohn's disease-like colitis. An aberrant, Th1-driven CD4$^+$ T-cell response to enteric bacteria seems to be important in the pathogenesis of this murine colitis. However, no specific bacteria or bacterial products have been identified, and whether the colitis is mediated by the activation of CD4$^+$ T cells that recognize specific peptide–MHC complexes is controversial. In this study, we analyzed the TCRβ chain complementarity determining region 3 length spectratype of colonic CD4$^+$ T cells isolated from diseased IL-10-deficient mice by using the Immunoscope technique. Screening of the diseased interleukin-10-deficient mice resulted in a restricted clonotype in TCR Vβ 13 and 14 subfamilies of colonic CD4$^+$ T cells. In contrast, a Gaussian distribution of clonotype of individual TCR Vβ subsets was observed in CD4$^+$ T cells from the peripheral lymphoid tissues. Although individual variability in the disease-related response was also noted in other IL-10-deficient mice maintained in La Jolla and Osaka, perhaps because of different stages of the disease, genetic background, or the housing environment, colitis-related public clones seemed to be shared in all the diseased mice tested. To address whether public clones were involved, we determined the DNA sequence of the clones. Public motifs were shared in colonic CD4$^+$ T cells from different background interleukin-10-deficient mice with colitis. The frequently found motifs were SXDWG and SATGNYAEQ. These motifs were not seen in the peripheral lymphoid tissues of diseased mice as well as the colon of nondiseased mice. Thus, the common motif may be related to a public gut-derived antigen, which could be important for the development of pathogenic CD4$^+$ T cells in this inflammatory bowel disease (IBD) model. The selection of Vβ-Jβ usage is perhaps stochastic in individual mice; however, the epigenetic generation of SXDWG motif by the recombination machinery and selection for this motif in the gut environment could be important for triggering IBD. © 2002 Elsevier Science (USA)

INTRODUCTION

Inflammatory bowel disease (IBD)[1] is a chronic, possibly noninfectious, inflammation limited to the large bowel (ulcerative colitis) or occurring anywhere along the gastrointestinal tract (Crohn's disease); the former is a relatively superficial, ulcerative inflammation, while the latter is a transmural, granulomatous inflammation. The major hypothesis concerning the pathogenesis of IBD is that the diseases are due to an abnormal and uncontrolled immune response to one or more normally occurring gut constituents (1–3). This hypothesis is based on the concept that immune homeostasis in the mucosal immune system relies on a delicate balance between the ability to react to potential gut pathogens and the ability not to react with common ubiquitous gut constituents (food antigens and bacterial flora). If the second arm of the balance mechanism, known as oral tolerance, is disturbed, and the mucosal system reacts with one or more common antigens in the mucosal environment, a condition is set up leading to chronic enterocolitis.

Evaluation of T-cell receptor diversity and clonality, in subjects who are going to be receiving vaccine or suffering from T-cell-mediated autoimmune disease, is critical for fully understanding the molecular basis of vaccine development and pathogenesis of autoimmune disease. In this regard, we and others have been studying the pathogenesis of IBD produced in TCR α chain-deficient mice (4, 5). It was shown that Th2-biased CD4$^+$ T cells expressing a TCR β-chain homodimer with a limited number of TCR Vβ subfamilies were increased in the diseased mice. Furthermore, clonotype analysis of the $\beta\beta$ T cells isolated from the diseased colon by using PCR-based single-strand conformation polymorphism (PCR-SSCP) analysis exhibited mono-

[1] Abbreviations used: aa, amino acid; CDR3, complementarity determining region 3; IBD, inflammatory bowel disease; IEL, intraepithelial lymphocyte; KO, knock-out; LP, lamina propria; MLN, mesenteric lymph nodes; PCR-SSCP, PCR single-strand conformation polymorphism.

1521-6616/02 $35.00

clonal or oligoclonal expansions. Thus, it was strongly suggested that the pathogenic ββ T cells were clonally accumulated upon stimulation with gut-derived specific antigens. In addition to this PCR–SSCP analysis, another sensitive and elegant tool for the evaluation of TCR repertoire diversity and clonal expansion is the "Immunoscope," originally developed by Kourilsky's laboratory at the Pasteur Institute (6–8).

IL-10 is well known as an anti-inflammatory cytokine that down-regulates macrophage and Th 1 cell function (9). The importance of IL-10 as a regulatory cytokine in the mucosal immune system is supported also by the evidence that mice genetically deficient for IL-10 spontaneously develop human Crohn's disease-like IBD with age (10). Another important finding concerning the regulatory role of IL-10 was clearly shown by the finding that cotransfer of a $CD4^+$, CD45 RB^{high} T-cell population isolated from IL-2 promoter-driven IL-10 transgenic mice, with the same pathogenic subset of T cells isolated from normal mice, significantly prevented the onset and reduced the severity of the colitis in the recipient SCID mice (11). Additional experiments by Powrie and co-workers have shown that the prevention of colitis by $CD4^+$, CD45 RB^{low} T cells requires IL-10 (12). The chronic enterocolitis which developed in the IL-10-deficient mice is mediated by $CD4^+$ T cells producing IFN-γ (13). In addition, adoptive transfer of Th1-biased $CD4^+$ T cells into SCID mice caused the colitis (14). It was also noted that germ-free IL-10 knock-out (KO) mice have no colitis, and resident enteric bacteria are necessary for the development of colitis in the mice (15). Although the involvement of the T cells for the development of colitis is clear, it is not known whether particular antigens from bacteria or other microorganisms play a role in disease induction.

To this end, several major questions in the IL-10-deficient murine colitis model remain to be elucidated: (i) Do the TCR repertoires of the mice with IBD share public specificities? (ii) Are the TCR repertoires unique in the colon? (iii) Where does the activation of T cells occur? To address these questions, an analysis of the TCR repertoire in murine colitis provides a powerful opportunity to characterize the pathogenic T-cell population (antigen-specificity, publicity, and distribution) in a manner not possible in studies on human patients (16). In this study we have analyzed TCR diversity of the pathogenic $CD4^+$ T cells in the colon of IL-10-deficient mice to assess the dissemination of the Ag-reactive T cells and the potential role of common bacterial constituents in colitis pathogenesis.

MATERIALS AND METHODS

Mice

IL-10-deficient mice with two different backgrounds, C57BL/6 × 129Ola mixed or C57BL/6, were purchased from The Jackson Laboratory (Bar Harbor, ME) and maintained at the La Jolla Institute for Allergy and Immunology and Osaka University, respectively. The C57BL/6 × 129Ola mixed-background IL-10-deficient mice were housed under specific pathogen-free conditions, whereas the C57BL/6-background IL-10-deficient mice were maintained under conventional conditions free of specific pathogens. All procedures were approved by the Animal Care and Utilization Committees at the respective institutions. Ages of the mice at the time of analysis are given under Results and Discussion.

Isolation of Lamina Propria Lymphocytes

Mucosal lymphocytes were isolated according to a published method (4, 5). Briefly, the large intestine was removed and carefully cleaned from the mesentery, opened longitudinally, and flushed of fecal content. The removed intestine was cut into 0.5-cm pieces, transferred into 50-ml Erlenmeyer flasks, and shaken three times at 200 rpm for 20 min each time at 37°C in HBSS without Ca^{2+} or Mg^{2+} and containing 1 mM DTT (Sigma, St. Louis, MO) to remove intestinal epithelial cells and intraepithelial lymphocytes. To isolate lamina propria lymphocytes, the remaining intestinal tissue was minced, transferred to 20-ml scintillation glass vials, and shaken for 30 min at 37°C in RPMI supplemented with 2% FBS containing collagenase at 0.5 mg/ml (Nitta Gelatin, Osaka, Japan). The cell suspensions were collected and passed through a glass fiber. The pelleted cells were passed over a Percoll gradient and processed as described (4). For purification of colonic $CD4^+$ T cells, the mononuclear cells were sorted with a FACSVantage flow cytometer (Becton Dickinson) after double labeling. PE-labeled anti-CD4 (L3T4) and FITC-labeled anti-TCRβ (H57-597) (PharMingen, San Diego, CA) were used in combination.

mRNA Extraction and cDNA Synthesis

mRNA was prepared using the QuickPrep micro mRNA purification kit (Pharmacia). The full quantity of mRNA obtained was used for single-strand cDNA synthesis. The mRNA was denatured for 10 min at 70°C and then incubated with oligo(dT)15 (5 μM), dNTPs (1 μM each), RNasin (40 U; Promega, Madison, WI), and AMV reverse transcriptase (2 U; Roche, Mannheim, Germany) in the supplier's buffer at 42°C for 1 h, followed by incubation at 72°C for 10 min.

PCR Amplifications, Primer Extensions, and Data Analysis

PCR amplification was conducted in 50 μl using 1/40 of the cDNA with 2 U of *Taq* polymerase (Perkin–

Elmer, Foster City, CA) in the supplier's buffer. Sense oligonucleotides specific for each of the 23 Vβ genes and antisense oligonucleotides for Cβ have been described (16). Forty cycles of PCR were conducted in a Perkin–Elmer 9600 Automate, with each cycle consisting of 94°C for 45 s, 60°C for 45 s, and 72°C for 45 s. Each PCR product was then used as a template for extension, or run-off, reactions with oligonucleotides labeled with a fluorescent tag. Fluorescent primers used included an internal Cβ primer and primers specific for each of the 12 Jβs (16). The fluorescent run-off products generated varied in size depending on complementarity determining region 3 (CDR3) length. Run-off products were subjected to capillary electrophoresis in an automated DNA sequencer (Applied Biosystems, Foster City, CA), and CDR3 size distribution and signal intensities were analyzed with GeneScan software (Perkin–Elmer). The patterns observed contained up to eight size peaks, each spaced by three nucleotides, corresponding to in-frame transcripts. The area under each peak was proportional to the quantity of TCR transcript of the corresponding CDR3 length in the sample.

Cloning and Sequencing of Selected Vβ-Jβ Rearrangements

Amplified PCR products were diluted 1/100 with H_2O, and 1 μl was used as a template for amplification of selected Vβ-Jβ rearrangements. PCR was performed with the reagents and quantities described above, using a sense oligonucleotide specific for the Vβ-chain of interest and an antisense oligonucleotide specific for the Jβ-chain of interest. Twenty-five cycles, each at 94°C for 45 s, 60°C for 45 s, and 72°C for 45 s, were completed in a GeneAmp 9600 PCR System (Perkin–Elmer). PCR products were analyzed on a 2% agarose gel stained with ethidium bromide to monitor the quality and quantity of the reaction products. Each Vβ-Jβ amplified product was then shotgun cloned with the pGEM-T Easy TA cloning kit (Promega, Madison, WI). Resulting colonies were randomly selected, and cultures were grown. Plasmid DNA was isolated from bacteria cultures using Wizard Plus Miniprep kits (Promega). Sequencing reactions were performed with an ABI Prism dRhodamine Terminator Cycle Sequencing Ready reaction kit (Perkin–Elmer) and analyzed on an automated sequencer.

RESULTS AND DISCUSSION

Immunoscope Analysis of TCR Vβ Clonotype Revealed Clonal Expansion of Pathogenic CD4⁺ T Cells in Diseased Colon

The first series of experiments was aimed at identifying expanded populations of $CD4^+$, TCR $V\beta^+$ cells that might be associated with IBD in IL-10 KO mice and to determine whether there is a unique TCR repertoire in the large intestine, the primary site of inflammation. To this end, RNAs extracted from FACS-purified $CD4^+$ T cells (100,000 cells) in the colonic lamina propria (LP) and mesenteric lymph node (MLN) of a diseased IL-10 KO mouse with anal prolapse (C57BL/6 and 129Ola mixed background) that was maintained at the animal facility of the La Jolla Institute for Allergy and Immunology (La Jolla IL-10-deficient mouse) were reverse-transcribed into cDNA. Aliquots were amplified by PCR with one of the Vβ1-Vβ20 primers and a Cβ-specific primer. The PCR products were then visualized by carrying out a run-off PCR with 6-FAM-labeled Cβ5 primer, and the fluorescent run-off products were loaded onto an ABI 310 Genetic Analyzer and analyzed using GeneScan software, which allowed determination of the fluorescence intensity of each band as well as its actual size. The absence of specific stimulation appears as a Gaussian-like distribution of the CDR3 sizes for a given Vβ-Jβ run-off. Specific antigenic stimulation leads to the expansion of single peaks.

As seen in Fig. 1, a typical Gaussian distribution of CDR3 lengths of individual TCR Vβ-Cβ PCR products was observed in the peripheral lymphoid tissue (MLN) of La Jolla IBD mouse 1, suggesting a polyclonal repertoire of T cells away from the site of disease. On the other hand, the TCR Vβ3, Vβ5.2, Vβ8.1, Vβ13, Vβ14, and Vβ18-Cβ PCR products in colonic $CD4^+$ T cells exhibited a bias of single peak of CDR3 length, while the TCR Vβ10 and Vβ12-Cβ product and the Vβ8.2-Cβ PCR product had two and three predominant CDR3 peaks in each case; this bias suggested a clonal expansion of the colonic $CD4^+$ T cells induced by stimulation with a particular antigen.

Expansions of a single predominant peak in the colonic LP were observed also in two other IL-10-deficient mice (La Jolla mice 2 and 3) with IBD that also had been maintained at La Jolla (Fig. 2). In La Jolla IBD mouse 2, the TCRVβ12 and Vβ14-Cβ PCR products exhibited a single peak of CDR3 length, while the TCR Vβ5.2 and Vβ10-Cβ PCR products were composed of two or three predominant peaks. In La Jolla IBD mouse 3, the TCR Vβ4, Vβ10, Vβ12, and Vβ14-Cβ products showed a predominant bias of CDR3 segment. These results strongly suggest that potentially pathogenic $CD4^+$ T cells were antigen-specifically and clonally infiltrated in the colon of IL-10 KO mice with colitis. It was interesting that there was some sharing of predominant CDR3 lengths (e.g., Vβ 14) among the different diseased IL-10-deficient mice bred in La Jolla.

The identical expanded peaks in the colonic LP were also found in the MLN T cells bearing a TCRβ chain exhibiting a Gaussian distribution of CDR3 segments (Fig. 1). Thus, it is not certain that any expanded peaks

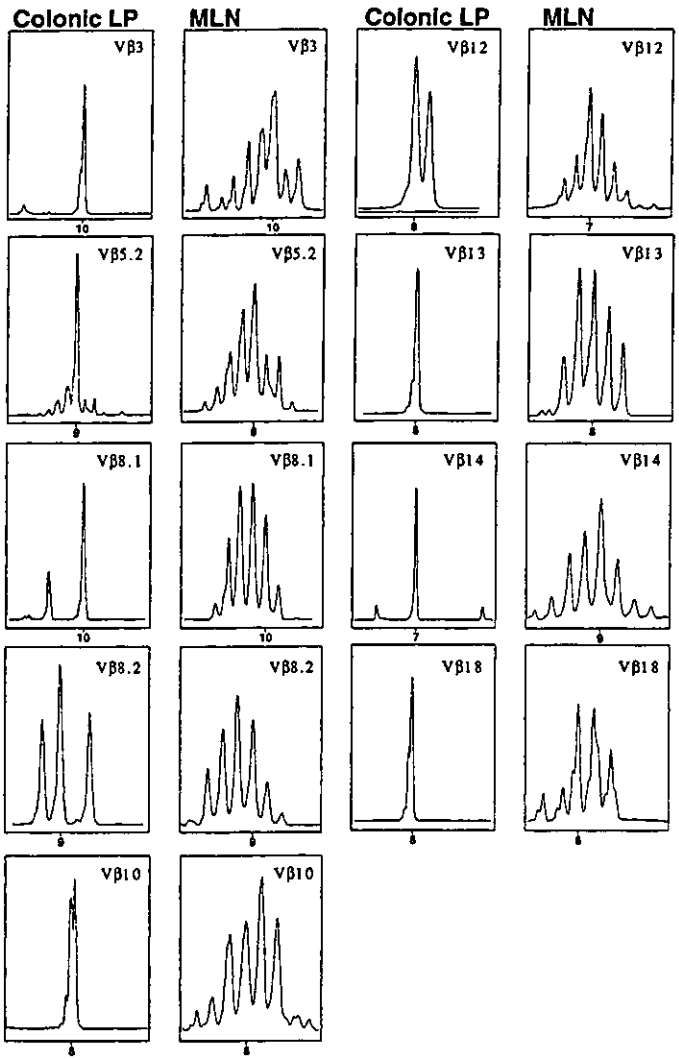

FIG. 1. Immunoscope analysis of TCR Vβ clonotype (CDR3β size distribution) of CD4⁺ T cells isolated from colonic LP and MLN of IL-10-deficient mouse 1 with IBD, which was maintained under specific pathogen-free conditions at the La Jolla Institute for Allergy and Immunology. CD4⁺ T cells were purified from the colonic LP and MLN of IL-10-deficient mouse 1 by cell sorting using FACSvantage. cDNA from the FACS-purified CD4⁺ T cells was subjected to PCR using particular Vβ- and Cβ-specific primers followed by a run-off with a nested fluorescent Cβ-specific primer. The CDR3β size distribution was analyzed with the GeneScan software program. Depicted are the CDR3 profiles from mouse 1 for selected Vβ-Cβ PCR amplification with the indicated Vβ primers. The intensity of fluorescence is presented in arbitrary units as a function of CDR3 length in amino acids, and a CDR3 length of particular aa is indicated. The peaks are spaced by 3 nucleotides.

that we have observed are really LP lymphocyte-specific, as opposed to being found in MLN and perhaps elsewhere. For example, the IL-10-deficient La Jolla mouse 1 has a predominant 9-amino-acid (aa) peak for Vβ 8.2 in the colonic Cβ run-off; there also is a 9-aa peak in the MLN. Although it is a small peak, it could represent the same clone. There is a limited recirculation of intestinal intraepithelial lymphocytes, and to a lesser extent LP lymphocytes (17, 18), such that once T cells are found in the intestine, they probably tend to stay there. Because migration outward, i.e., from the intestine to the systemic lymphoid tissue, is unlikely, the finding of common expanded peaks in the intestine (colonic LP) and MLN leads to the hypothesis that the initial T cell activation may occur outside the colonic LP. Perhaps dendritic cells in the mucosa systemically transport bacterial or other relevant gut-derived antigens (19–21). On the other hand, it was shown that a subset of LP lymphocytes enter the recirculating lymphocyte pool, e.g., thoracic duct, while over 70% of the LP lymphocytes are composed of the continual entry of cells from the common lymphocyte pool (17, 22).

Development of Pathogenic CD4⁺ T Cells with Oligoclonal/Public Clones in Different IL-10-Deficient Mice with IBD

We further performed the spectratype analysis of the TCR Vβ repertoire by using IL-10 KO mice with a different genetic background (C57BL/6) and from conventional housing conditions free of specific pathogens in order to address two issues: (i) Are there common clones in different IL-10-deficient mice? (ii) Are normal LP lymphocytes as oligoclonal as are those in IL-10-deficient mice? Thus, we purified CD4⁺ T cells by FACS from IL-10 KO mice (Osaka-1 and Osaka-2) with colitis, IL-10 KO mice (Osaka-3 and Osaka-4) without IBD, and normal C57BL/6 mice. Three sets of immunoscope analysis were done by using Cβ, Jβ 2.1, and Jβ 2.4 run-offs. We chose the Jβ2.1 and Jβ2.4 from 12 kinds of Jβ subfamilies based on our previous study that Jβ2.1 and Jβ2.4 were dominantly used in the pathogenic T-cell clones in TCR-α chain-deficient mice with IBD (5). In addition, when dominant subsets (TCR Vβ6, Vβ8.1/8.2, and Vβ14) of the CD4⁺ T cells isolated from the colonic LP of diseased Osaka IL-10-deficient mice were analyzed for the CDR3 TCRβ distribution with all 12 Jβ primers, Jβ2.1- and Jβ2.4-Cβ run-offs preferentially gave clonal skewing peaks (data not shown). This was the additional rationale for the selection of particular Jβ2.1 and Jβ2.4 in the following run-off analysis.

Although the results were complicated due to individual variability in the disease progression, several disease-related public clones were present in the colons of IL-10-deficient Osaka mouse 1 and Osaka mouse 2 with IBD (Fig. 3). Distinct colitis-related private clones were noted also in the individual diseased mice (Fig. 3).

A Gaussian distribution of CDR3 lengths was observed in all the Vβ and Cβ run-off products of the colonic as well as peripheral MLN CD4⁺ T cells isolated from IL-10-deficient Osaka mouse 1 with IBD,

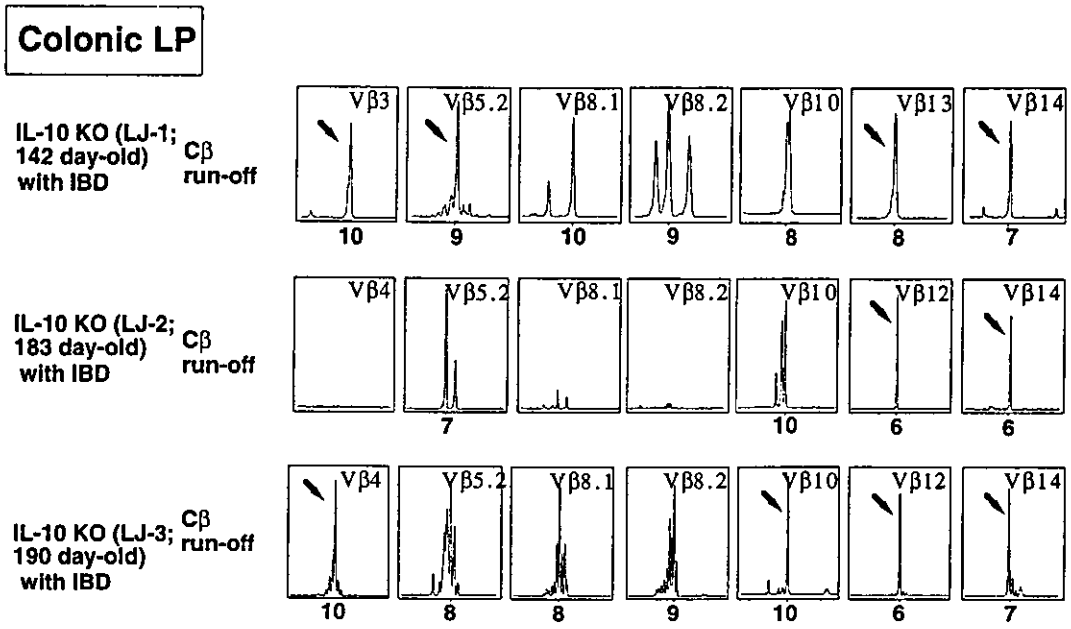

FIG. 2. CDR3β size distribution among colonic CD4⁺ T cells isolated from different IL-10-deficient mice with IBD. C57BL/6 × 129Ola mixed-background IL-10-deficient mice with IBD were maintained under specific pathogen-free conditions at the La Jolla Institute for Allergy and Immunology. The Immunoscope analysis was performed as described in the legend of Fig. 1. Depicted are the CDR3 profiles from IL-10-deficient mice 1, 2, and 3 for selected Vβ-Cβ PCR amplification with the indicated Vβ primers. Arrows indicate expansions discussed in the text. The intensity of fluorescence is presented in arbitrary units as a function of CDR3 length in amino acids, and a CDR3 length of particular aa is indicated. The peaks are spaced by 3 nucleotides.

which was maintained in a conventional animal facility (Fig. 3). However, when particular Jβ run-offs were performed, the Gaussian distribution of CDR3 sizes for the colonic Vβ-Cβ run-off did not reflect the true diversity of the response in the IL-10 KO Osaka mouse 1 with IBD. Clonal expansion of the CDR3 region was observed in the colonic Vβ10-Jβ2.1 and Vβ13-Jβ2.1 run-off of Osaka mouse 1. The predominant peaks bore TCR lengths of 9 aa, in the CDR3 region. In addition, when a Jβ2.4 run-off was performed, a single predominant CDR3 region peak was detected for the Vβ8.2 and Vβ13 subsets of colonic CD4⁺ T cells from Osaka mouse 1, composed of 10- and 6-amino-acid CDR3 region lengths, respectively. The paucity of clones in Jβ run-offs for the colonic CD4⁺ T cells was also observed in Osaka IL-10 KO mouse 2 with IBD. Clonal skewing of CDR3 length was noted in the colonic Vβ8.1-Jβ2.1 (9 aa), Vβ8.2-Jβ2.1 (9 aa), Vβ13-Jβ2.1 (9 aa), Vβ14-Jβ2.1 (6 aa), Vβ13-Jβ2.4 (9 aa), and Vβ14-Jβ2.4 (9 aa).

There seemed to be a tendency for the colonic LP lymphocytes of IL-10-deficient mice (Osaka 1 and Osaka 2) with IBD to have reduced diversity compared to LP lymphocytes of the IL-10-deficient mice without IBD (Osaka-3 and Osaka-4) and wild-type C57BL/6 mice. No obvious clonal expansion was seen for nondiseased IL-10-deficient as well as wild-type C57BL/6 mice in the CDR3 size profile for each Vβ-Cβ PCR product. In addition, analysis of Jβ run-offs of colonic CD4⁺ T cells in nondiseased IL-10-deficient and C57BL/6 mice confirmed their polyclonality, as the CDR3 size distribution for each Jβ primer extension reaction was also Gaussian. However, expansion of some Vβ-Jβ combinations was occasionally observed in colonic LP of IL-10 KO Osaka mice without IBD and wild-type C57BL/6 mice (such as the Vβ14-Jβ2.4 combination in IL-10 KO Osaka-3 and the Vβ10-Jβ2.4 combination in C57BL/6 mice). These scattered expansions were not disease-related since they did not have sequence homology to the disease-related clone (see below). Thus, they may reflect individual responses to antigens irrelevant to IBD, although their role in IBD is not excluded.

Another interesting finding, and the most striking, is the sharing of predominant CDR3 lengths between the two different diseased IL-10 KO Osaka mice for the Jβ2.1 and Jβ2.4 run-offs. For Jβ2.1, there is concordant Vβ13 (9 amino acids). For Jβ2.4, there are shared peaks of Vβ13 (9 aa). This seems to be a higher degree of sharing or public specificities than was seen in the CD4⁺, CD45RB^{high} T cell transfer model (16). It is conceivable that a model that takes months to develop IBD, such as IL-10 KO mice, might select for public clones less than in the more acute model of disease that results from CD4⁺, CD45RB^{high} cell transfer (16). Furthermore, in animals with an intact immune system, there is probably more regulation by other T cells and

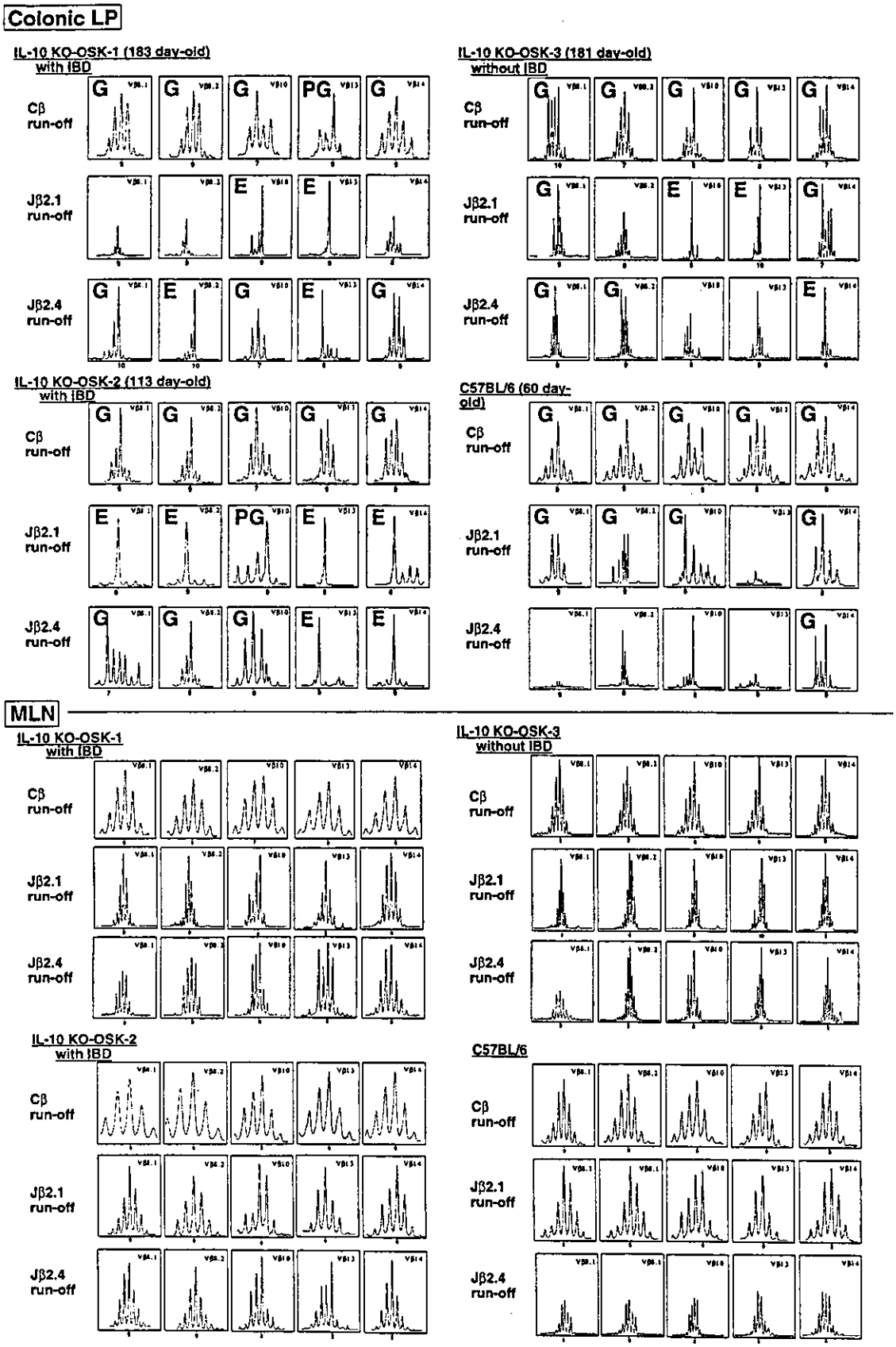
Colonic LP
IL-10 KO-OSK-1 (183 day-old) with IBD
IL-10 KO-OSK-3 (181 day-old) without IBD
IL-10 KO-OSK-2 (113 day-old) with IBD
C57BL/6 (60 day-old)
Cβ run-off
Jβ2.1 run-off
Jβ2.4 run-off
MLN
IL-10 KO-OSK-1 with IBD
IL-10 KO-OSK-3 without IBD
IL-10 KO-OSK-2 with IBD
C57BL/6

selection for particular clones (23–27). When T cells are placed into an immune-deficient animal, they first undergo homeostatic proliferation to fill the "empty" space of the immune organs (28). Thus, the CD45RB^{high} transfer model would give a different result from spontaneous models, including the IL-10-deficient mice.

In contrast, there is a relatively low level of sharing of the TCR repertoire in unimmunized inbred mice (29), a finding which might be due to stochastic elements in the antigen receptor gene rearrangement and selection processes. In addition to differences in the naive repertoire, small differences in the time of encounter with antigen may be critical to the preferential expansion of particular T cell clones (30).

Determination of the DNA Sequence of the Predominant Clones That Were Shared in Diseased IL-10-Deficient Mice

There seemed to be a shared skewing of the CDR3 TCR length among the different diseased IL-10 mice bred in La Jolla (B6 and 129 mixed background) and Osaka (B6 background). To this end, we selected the expanded Vβ-Jβ$^+$, CD4$^+$ colonic T-cell populations as well as corresponding MLN T-cell populations as candidates for IBD-associated expansions of particular T cells at the onset of the disease. The populations were as follows: (i) La Jolla IBD mouse 1; Vβ12-Jβ2.4 and Vβ13-Jβ2.1 in colonic and MLN CD4$^+$T cells. (ii) La Jolla mouse 2; Vβ10-Jβ2.1, Vβ11-Jβ2.1, and Vβ12-Jβ2.4 in colonic and MLN CD4$^+$ T cells. (iii) La Jolla IBD mouse 3; Vβ8.2-Jβ2.4, Vβ10-Jβ2.1, Vβ12-Jβ2.4, and Vβ14-Jβ2.4 in colonic and MLN CD4$^+$ T cells. (iv) Osaka IBD mouse 1; Vβ8.2-Jβ2.4, Vβ13-Jβ2.1, and Vβ14-Jβ2.4 in colonic and MLN CD4$^+$ T cells. (v) Osaka IBD mouse 2; Vβ8.1-Jβ2.1, Vβ8.2-Jβ2.4, Vβ13-Jβ2.1, Vβ13-Jβ2.4, and Vβ14-Jβ2.4 in colonic and MLN CD4$^+$ T cells. (vi) Osaka IL-10 mouse 3 without IBD; Vβ10-Jβ2.1, Vβ13-Jβ2.1, and Vβ14-Jβ2.4 in colonic and MLN CD4$^+$ T cells. (vii) Osaka IL-10 mouse 4 without IBD; Vβ8.2-Jβ2.4, Vβ13-Jβ2.1, and Vβ14-Jβ2.4 in colonic and MLN CD4$^+$ T cells. We then determined DNA sequences to identify public clones, i.e., clones shared between Osaka and La Jolla IL-10 KO mice with IBD. Eight to 36 clones were analyzed for DNA sequence for each amplified Vβ-Jβ combination.

As shown in Figs. 4A and 4B, some public CDR3 motifs were shared between colonic CD4$^+$ T cells isolated from IL-10-deficient mice with IBD maintained in Osaka and those maintained in La Jolla. The most frequently shared motif was SXDWG, which was shared in the La Jolla IBD mouse 1 (Vβ13-Jβ2.1) at a frequency of 12/12 (Fig. 4A), La Jolla IBD mouse 2 (Vβ10-Jβ2.1) at 4/8 (Fig. 4A), La Jolla IBD mouse 3 (Vβ10-Jβ2.1) at 14/24 (Fig. 4A), Osaka IBD mouse 1 (Vβ8.2-Jβ2.4 at 3/7 and Vβ14-Jβ2.4 at 5/14; Fig. 4B), and Osaka IBD mouse 2 (Vβ13-Jβ2.4 at 2/23 and Vβ14-Jβ2.4 at 1/21; Fig. 4B). Another interesting public motif was SATGNYAEQ, which was shared in the Osaka IBD mouse 1 (Vβ13-Jβ2.1) at 30/33 (Fig. 4B) and Osaka mouse 2 (Vβ13-Jβ2.1) at 12/27 (Fig. 4B).

These shared motifs were not seen in the peripheral lymphoid tissues, i.e., MLN of either the diseased La Jolla or Osaka mice (Figs. 4A and 4B). Finally, it was important to confirm that the motifs were not seen in the nondiseased IL-10 KO mice in order to determine whether the motifs were truly IBD-specific. As shown in Fig. 4C, the SXDWG and SATGNYAEQ motifs were not seen in the colons and MLN of nondiseased IL-10-deficient Osaka mouse 3 and Osaka mouse 4. Thus, the common motifs might see a public gut-derived antigen which is important for the development of pathogenic CD4$^+$ T cells in this colitis model. In terms of an SXDWG motif using a flexible Vβ-Jβ rearrangement, it may be that an epitope drives the onset of IBD. In this regard, it was reported that mice lacking the TCR Vγ5 chain retained a conformational determinant by using "shuffled TCR γ chain" (31). In our case, the selection of Vβ-Jβ usage is perhaps stochastic in individual mice; however, the epigenetic generation of the SXDWG motif in different Vβ-Dβ-Jβ combinations by recombination machinery followed by selection in the gut environment could be crucial for the triggering of IBD.

It is possible that the public motifs SXDWG and (or) SATGNYAEQ are derived from commensal bacterial antigens. In support of this view, it has been reported that IL-10-deficient mice housed under germ-free conditions remained healthy, while those housed under conventional and SPF conditions developed colitis after weaning (10, 32). In addition, the data obtained from a CD4$^+$, CD45RB^{high} T-cell adoptive transfer model with reduced flora-bearing SCID mice suggest that bacteria

FIG. 3. Comparison of CDR3β size distribution of CD4$^+$ T cells isolated from colonic lamina propria and mesenteric lymph nodes of IL-10-deficient mice with IBD with those of IL-10-deficient mice without IBD and wild-type C57BL/6 mice. C57BL/6 background IL-10-deficient mice were maintained under conventional conditions at the animal facility of Osaka University. The Immunoscope analysis was performed as described in the legend of Fig. 1. Depicted are the CDR3 profiles for selected Vβ-Cβ, Vβ-Jβ2.1, and Vβ-Jβ2.4 PCR amplifications with the indicated Vβ primers. One representative of two different mice is shown both in IL-10-deficient mice without IBD and in C57BL/6 mice. E indicates expansions discussed in the text. G and PG mean Gaussian-type and pseudo-Gaussian-type distribution of the CDR TCR β length, respectively. The intensity of fluorescence is presented in arbitrary units as a function of CDR3 length in amino acids, and a CDR3 length of particular aa is indicated. The peaks are spaced by 3 nucleotides.

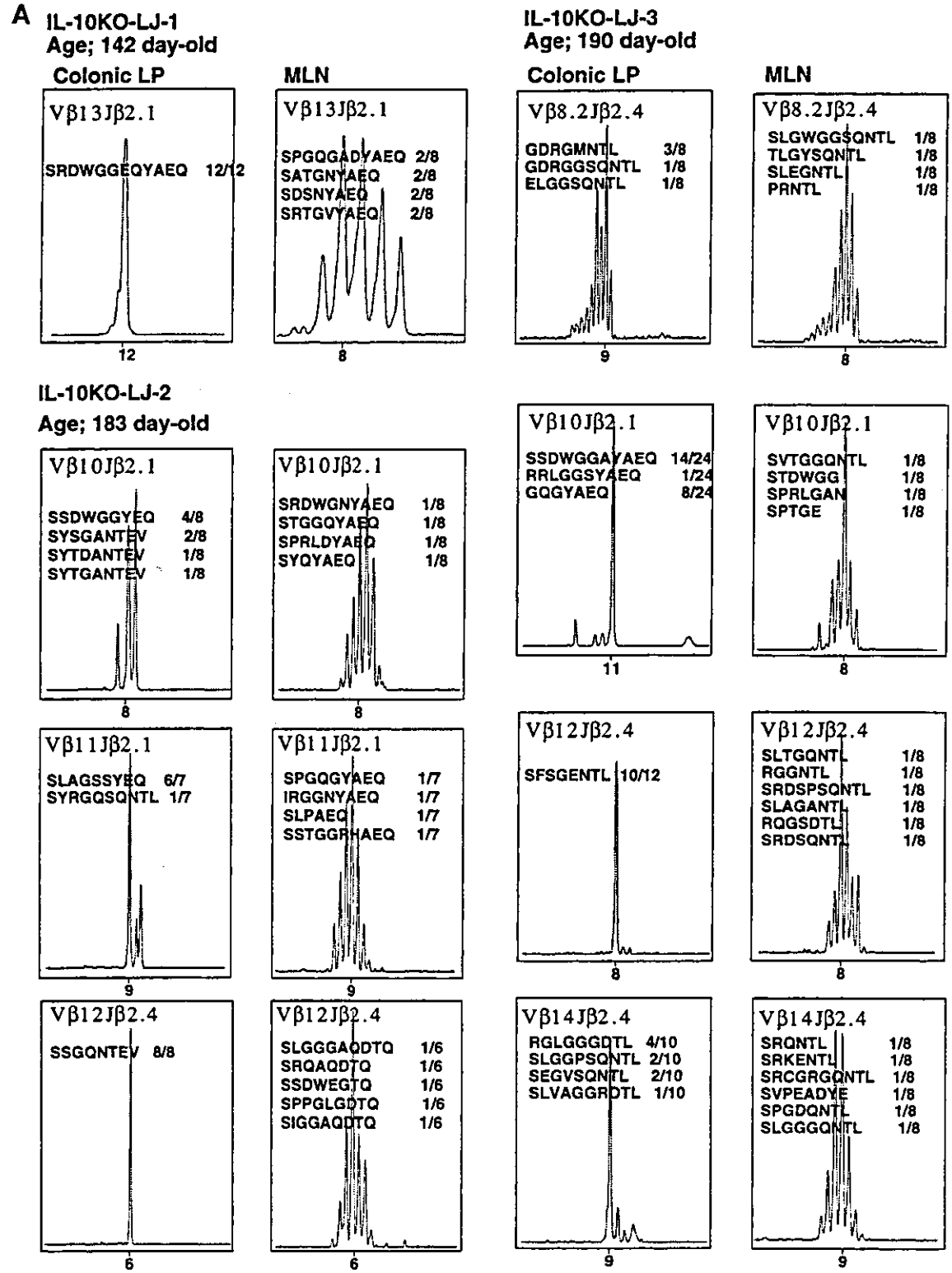

FIG. 4. (A–C) Identical clones can be found throughout the colonic LP of different IL-10-deficient mice with IBD. Translated amino acid sequences of expanded clones in colonic LP and their counterparts in respective MLN are shown. Amplifications were done using the indicated Vβ and Jβ primers from the indicated IL-10-deficient mice with or without IBD. Primers pairs were chosen based on fragment length analysis showing the presence of a predominant Vβ-Jβ CDR3β length in colonic LP. However, the Vβ-Jβ amplification products were shotgun-cloned without any selection for rearrangements of the predominant size. The predominant or expanded sequence is indicated, and the detection frequencies are determined by the number of sequences with the listed CDR3 sequence out of the total number of sequences generated for the particular Vβ-Jβ combination in the mouse indicated.

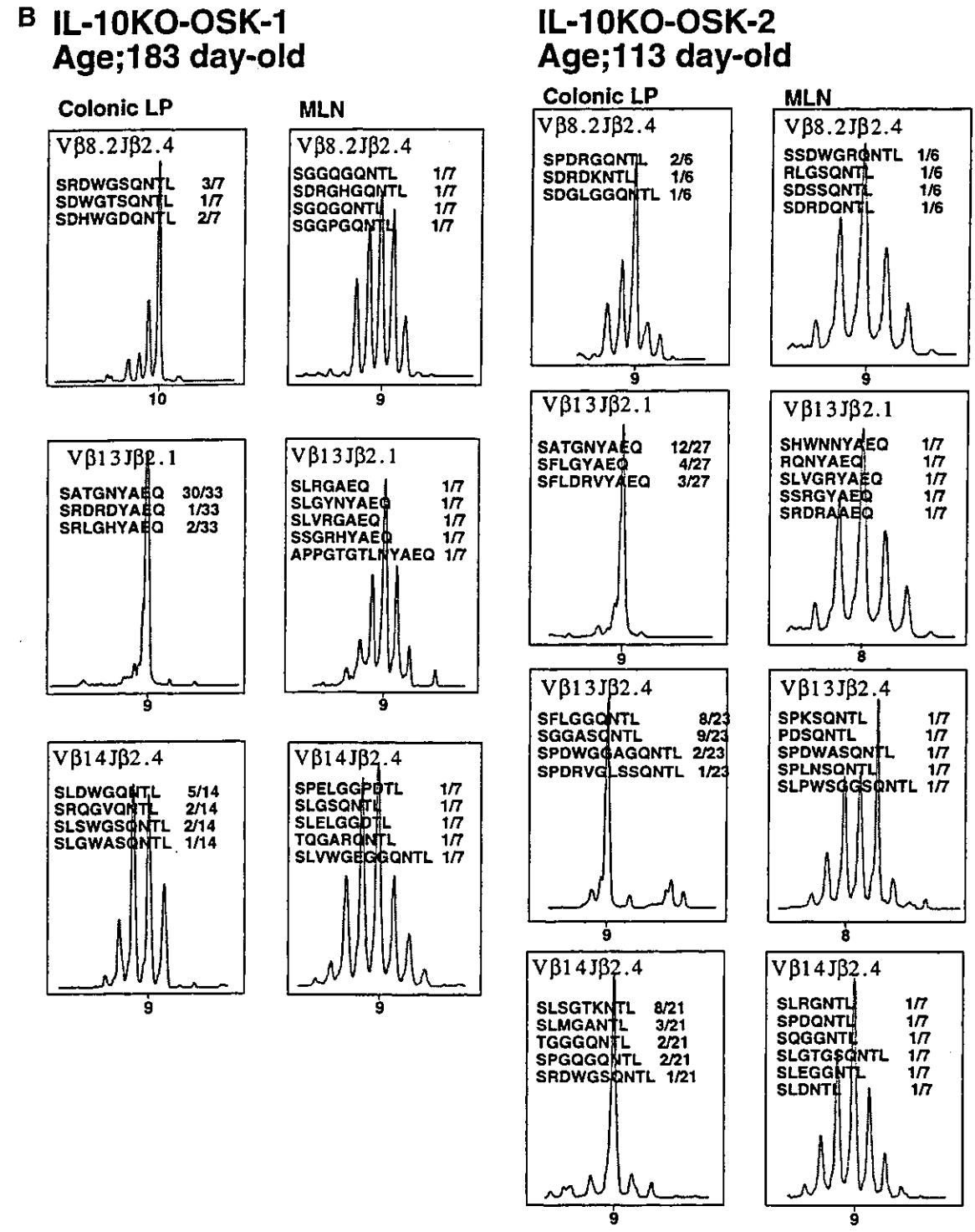

FIG. 4—*Continued*

or bacterial products likely are important in the more rapid kinetics of homing of pathogenic T cells to the large intestine, their subsequent expansion, and the enhanced susceptibility of the large intestine to inflammation (33). Thus, additional experiments will be required to determine what particular antigens from bacteria or other microorganisms mediate the development of the pathogenic T cells and drive the onset of the colitis. Otherwise, because bacteria also can stimulate inflammatory cytokines and chemokine secretion by intestinal

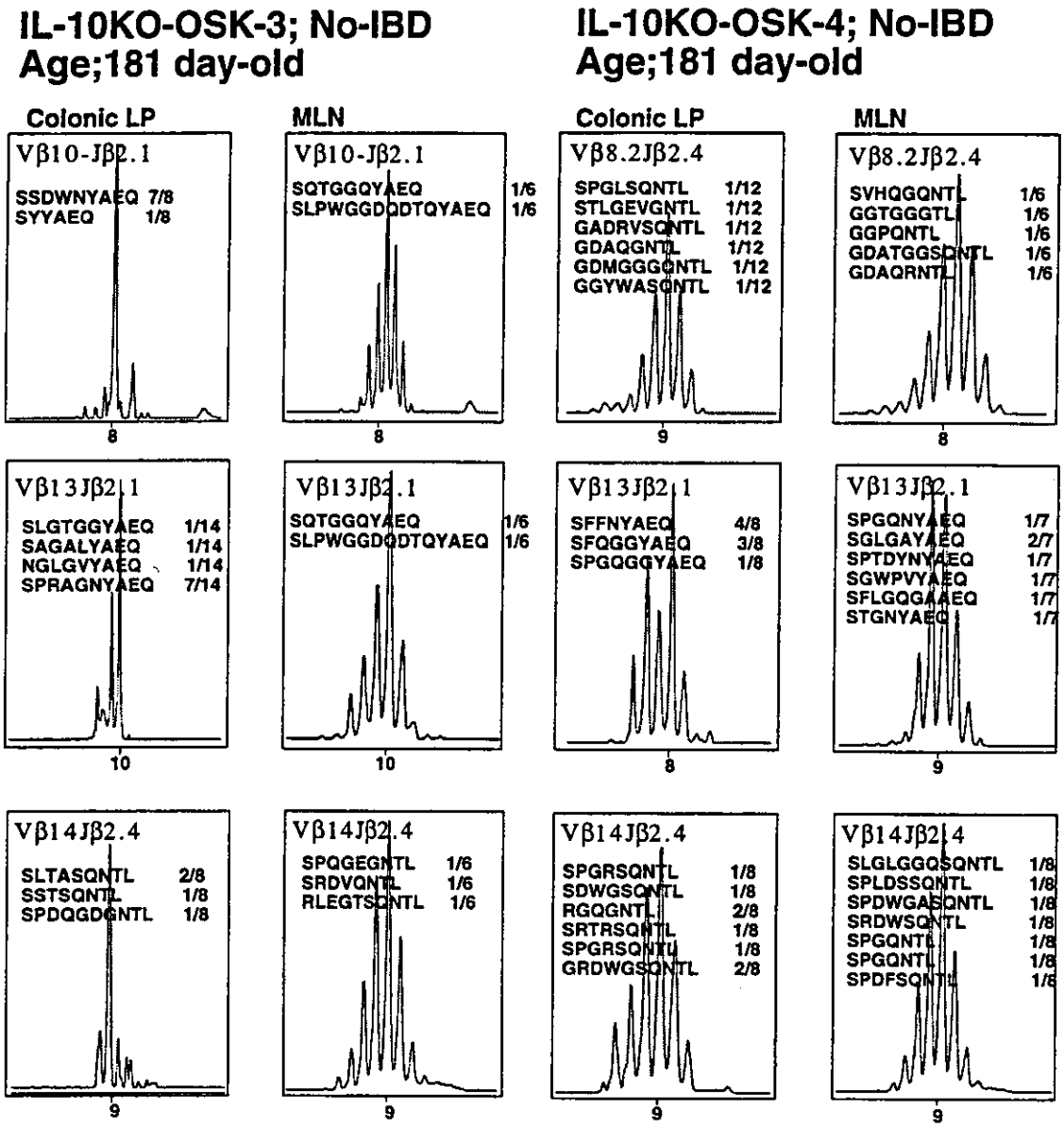

FIG. 4—*Continued*

epithelial cells (34), the presence of a higher bacterial load in the large intestine may provide a non-Ag conditioning factor that makes the intestinal tissue more susceptible to colonizing by T lymphocytes with a variety of specificities.

It is intriguing that public clones were present in the IL-10-deficient mice from both Osaka and La Jolla. Although the frequency of the public motif found in the diseased sites was variable, it is still possible that an identical/common antigen is involved in the murine model. If one can identify these clones from the peripheral blood as well (using CDR3-specific primers), one could predict the time to disease onset by clonal analysis. Furthermore, it is important to determine whether this clone drives disease onset or whether this clonal expansion is a product of the disease. If the clonal expansion of a public clone is causative, transfer of this clone should induce the disease in recipient animals.

Analyses of human IBD have provided some evidence for shared clones in peripheral blood $CD4^+$ T lymphocytes of identical twins concordant for Crohn's disease (35) and for shared sequence motifs in activated $CD4^+$ and/or $CD8^+$ T cells of the intestinal mucosa from unrelated individuals with IBD (36). Similar to the results from our analysis of diseased mice, however, in all these cases private or individual TCR expansions greatly outnumber the public clones identified.

Although the bacterial microflora may be important in disease pathogenesis (37), not all bacteria have the same capacity to induce inflammation. Some bacteria that are considered to be probiotics, such as the various *Lactobacillus* species, prevent colitis from occurring in IL-10-deficient animals living under specific pathogen-free conditions (38). On the other hand, *Helicobacter hepaticus* caused colitis when introduced into pathogen-free IL-10-deficient mice and not in immune-competent controls (39).

Sutton *et al.* (40) recently isolated a novel microbial I2 antigen by using representational difference analysis. Bacterial 12 antigen was specifically localized to mucosal lesions in human Crohn's disease. *In vitro* $CD4^+$ T-cell proliferation and cytokine assays revealed that there were memory $CD4^+$ T-cell responses to bacterial I2 antigen in murine IBD models, including IL-10-deficient and TCR α-chain-deficient mice (41). Although those workers have not done repertoire studies on I2-reactive T cells, it will be of interest to learn whether I2-reactive T cells have the public motifs SXDWG or SATGNYAEQ.

ACKNOWLEDGMENTS

This study was supported, in part, by Grants-in-Aid for Scientific Research from the Ministry of Education, Science, Sports, and Culture of Japan, and the Ministry of Health and Welfare of Japan. The authors thank Dr. William R. Brown (Denver VA Medical Center) for his helpful comments and editorial assistance.

REFERENCES

1. Powrie, F., T cells in inflammatory bowel disease: Protective and pathogenic roles. *Immunity* **3,** 171–174, 1995.
2. Blumberg, R. S., Saubermann, L. J., and Strober, W. Animal models of mucosal inflammation and their relation to human inflammatory disease. *Curr. Opin. Immunol.* **11,** 648–656, 1999.
3. DeWinter, H., Cheroutre, H., and Kronenberg, M., The yin and yang of T cells in intestinal inflammation: Pathogenic and protective roles in a mouse colitis model. *Am. J. Pathol.* **276,** G1317–1321, 1999.
4. Takahashi, I., Iijima, H., Katashima, R., Itakura, M., and Kiyono, H., Clonal expansion of $CD4^+$ TCR $\beta\beta^+$ T cells in TCR α-chain deficient mice by gut-derived antigens. *J. Immunol.* **162,** 1843–1850, 1999.
5. Mizoguchi, A., Mizoguchi, E., Saubermann, L. J., Higaki, K., Blumberg, R. S., and Bhan, A. K., Limited CD4 T-cell diversity associated with colitis in T-cell receptor α mutant mice requires a T helper 2 environment. *Gastroenterology* **119,** 983–995, 2000.
6. Cibotti, R., Cabaniols, J. P., Pannetier, C., Delarbre, C., Vergnon, I., Kanellopoulos, J. M., and Kourilsky, P., Public and private Vβ T cell receptor repertoires against hen egg white lysozyme (HEL) in nontransgenic versus HEL transgenic mice. *J. Exp. Med.* **180,** 861–872, 1994.
7. Musette, P., Bequet, D., Delarbre, C., Gachelin, G., Kourilsky, P., and Dormont, D., Expansion of a recurrent Vβ5.3$^+$ T-cell population in newly diagnosed and untreated HLA-DR2 multiple sclerosis patients. *Proc. Natl. Acad. Sci. USA* **93,** 12461–12466, 1996.
8. Pannetier, C., Even, J., and Kourilsky, P., T-cell repertoire diversity and clonal expansions in normal and clinical samples. *Immunol. Today* **16,** 176–181, 1995.
9. Moore, K. W., O'Garra, A., deWaal Malefyt, R., Vieira, P., and Mossman, T. R., Interleukin-10. *Annu. Rev. Immunol.* **11,** 165–190, 1993.
10. Kuhn, R., Lohler, J., Rennnick, D., Rajewsky, K., and Muller, W., Interleukin-10-deficient mice develop chronic enterocolitis. *Cell* **75,** 263–274, 1993.
11. Hagenbaugh, A., Sharma, S., Dubinett, S. M., Wei, S. H. Y., Aranda, R., Cheroutre, H., Fowell, D. J., Binder, S., Tsao, B., Locksley, R. M., Moore, K. W., and Kronenberg, M., Altered immune responses in interleukin 10 transgenic mice. *J. Exp. Med.* **185,** 21011–21010, 1997.
12. Asseman, C., Mauze, S., Leach, M. W., Coffman, R. L., and Powrie, F., An essential role for interleukin 10 in the function of regulatory T cells that inhibit intestinal inflammation. *J. Exp. Med.* **190,** 995–1004, 1999.
13. Berg, D. J., Davidson, N., Kuhn, R., Muller, W., Menon, S., Holland, G., Thompson-Snipes, L., Leach, M. W., and Rennick, D., Enterocolitis and colon cancer in interleukin-10-deficient mice are associated with aberrant cytokine production and $CD4^+$ TH1-like responses. *J. Clin. Invest.* **98,** 1010–1020, 1996.
14. Davidson, N. J., Leach, M. W., Fort, M. M., Thompson-Snipes, L., Kuhn, R., Muller, W., Berg, D. J., and Rennick, D. M., T helper cell 1-type $CD4^+$ T cells, but not B cells, mediate colitis in interleukin 10-deficient mice. *J. Exp. Med.* **184,** 241–251, 1996.
15. Sellon, R., Tonkonogy, S., Schultz, M., Dieleman, L. A., Grenther, W., Balish, E., Rennick, D. M., and Sartor, R. B., Resident enteric bacteria are necessary for development of spontaneous colitis and immune system activation in interleukin-10-deficient mice. *Infect. Immun.* **66,** 5224–5231, 1998.
16. Matsuda, J., Gapin, L., Sydra, B. C., Byrne, F., Binder, S., Kronenberg, M., and Aranda, R., Systemic activation and antigen-driven oligoclonal expansion of T cells in a mouse model of colitis. *J. Immunol.* **164,** 2797–2806, 2000.
17. Poussier, P., Edouard, P., Lee, C., Binnie, M., and Julius, M., Thymus-independent development and negative selection of T cells expressing T cell receptor $\alpha\beta$ in the intestinal epithelium: Evidence for distinct circulation patterns of gut- and thymus-derived T lymphocytes. *J. Exp. Med.* **176,** 187–199, 1992.
18. Camerini, V., Panwala, C., and Kronenberg, M., Regional specialization of the mucosal immune system: Intraepithelial lymphocytes of the large intestine have a different phenotype and function than those of the small intestine. *J. Immunol.* **151,** 1765–1776, 1993.
19. Iwasaki, A., and Kelsall, B. L. Freshly isolated Peyer's patch, but not spleen, dendritic cells produce interleukin 10 and induce the differentiation of T helper type 2 cells. *J. Exp. Med.* **190,** 229–239, 1999.
20. Iwasaki, A., and Kelsall, B. L., Localization of distinct Peyer's patch dendritic cell subsets and their recruitment by chemokines macrophage inflammatory protein (MIP)-3α, MIP-3β, and secondary lymphoid organ chemokine. *J. Exp. Med.* **191,** 1381–1394, 2000.
21. Cook, D. N., Prosser, D. M., Forster, R., Zhang, J., Kuklin, N. A., Abbondanzo, S. J., Niu, X-D., Chen, S-C., Manfra, D. J., Wiekowski, M. T., Sullivan, L. M., Smith, S. R., Greenberg, H. B., Narula, S. K., Lipp, M., and Lira, S. A., CCR6 mediates dendritic cell localization, lymphocyte homeostasis, and immune responses in mucosal tissue. *Immunity* **12,** 495–503, 2000.
22. Arstila, T., Arstila, T. P., Calbo, S., Selz, F., Malassis-Seris, M., Vassalli, P., Kourilsky, P., and Guy-Grand, D., Identical T cell clones are located within the mouse gut epithelium and lamina

propria and circulate in the thoracic duct lymph. *J. Exp. Med.* **191,** 823–834, 2000.

23. Groux, H., O'Garra, A., Bigler, M., Rouleau, M., Antonenko, S., de Vries, J. E., and Roncarolo, M. G., A CD4$^+$ T-cell subset inhibits antigen-specific T-cell responses and prevents colitis. *Nature* **389,** 737–742, 1997.
24. Kronenberg, M., and Cheroutre, H., Do mucosal T cells prevent intestinal inflammation? *Gastroenterology* **118,** 974–977, 2000.
25. Poussier, P., Ning, T., Chen, J., Banerjee, D., and Julius, M., Intestinal inflammation observed in IL-2R/IL-2 mutant mice is associated with impaired intestinal T lymphopoiesis. *Gastroenterology* **118,** 880–891, 2000.
26. Boismenu, R., Natural and pharmacological strategies for the protection of mucosal surfaces. *Mucosal Immunol. Update* **8,** 5–9, 2000.
27. Saubermann, L. J., Beck, P., DeJong, Y. P., Pitman, R. S., Ryan, M. S., Kim, H. S., Exley, M., Snapper, S., Balk, S. P., Hagen, S. J., Kanauchi, O., Motoki, K., Sakai, T., Terhorst, C., Koezuka, Y., Podolsky, D. K., and Blumberg, R. S., Activation of natural killer T cells by α-galactosylceramide in the presence of CD1d provides protection against colitis in mice. *Gastroenterology* **119,** 119–128, 2000.
28. Ernst, B., Lee, D-S., Chang, J. M., Sprent, J., and Surh, C. D., The peptide ligands mediating positive selection in the thymus control T cell survival and homeostatic proliferation in the periphery. *Immunity* **11,** 173–181, 1999.
29. Bousso, P., Casrouge, A., Altman, J. D., Haury, M., Kanellopoulos, J., Abastado, J. P., and Kourilsky, P., Individual variations in the murine T cell response to a specific peptide reflect variability in naive repertoires. *Immunity* **9,** 169–178, 1998.
30. Bousso, P., Levraud, J. P., Kourilsky, P., and Abastado, J. P., The composition of a primary T cell response is largely determined by the timing of recruitment of individual T cell clones. *J. Exp. Med.* **189,** 1591–1600, 1999.
31. Mallick-Wood, C. A., Lewis, J. M., Richie, L. I., Owen, M. J., Tigelaar, R. E., and Hayday, A. C., Conservation of T cell receptor conformation in epidermal $\gamma\delta$ cells with disrupted primary Vγ gene usage. *Science* **279,** 1729–1733, 1998.
32. Song, F., Ito, K., Denning, T. L., Kuninger, D., Papaconstantinou, J., Gourley, W., Klimpel, G., Balish, E., Hokanson, J., and Ernst, P. B., Expression of the neutrophil chemokine KC in the colon of mice with enterocolitis and by intestinal epithelial cell line: Effects of flora and proinflammatory cytokines. *J. Immunol.* **162,** 2275–2280, 1999.
33. Aranda, R., Sydra, B. C., McAllister, P. L., Binder, S. W., Yang, H. Y., Targan, S. R., and Kronenberg, M., Analysis of intestinal lymphocytes in mouse colitis mediated by transfer of CD4$^+$, CD45RB^{high} T cells to SCID recipients. *J. Immunol.* **158,** 3464–3473, 1997.
34. Jung H. C., Eckman, L., Yang, S. K., Panja, A., Fierer, J., Morzycka-Wroblewska, E., and Kagnoff, M. F., A distinct array of proinflammatory cytokines is expressed in human colon epithelial cells in response to bacterial invasion. *J. Clin. Invest.* **95,** 55–65, 1995.
35. Probert, C. S., Chott, A., Turner, J. R., Saubermann, L. J., Stevens, A. C., Bodinaku, K., Elson, C. O., Balk, S. P., and Blumberg, R. S., Persistent clonal expansions of peripheral blood CD4 lymphocytes in chronic inflammatory bowel disease. *J. Immunol.* **157,** 3183–3191, 1996.
36. Saubermann, L. J., Probert, C. S., Christ, A. D., Chott, A., Turner, J. R., Stevens, A. C., Balk, S. P., and Blumberg, R. S., Evidence of T cell receptor β-chain patterns in inflammatory and noninflammatory bowel disease states. *Am. J. Physiol.* **276,** G613–G621, 1996.
37. Cong, Y., Brandwein, S. L., McCabe, R. P., Lazenby, A., Birkenmeier, E. H., Sundberg, J. P., and Elson, C. O. CD4$^+$ T cells reactive to enteric bacterial antigens in spontaneously colitic C3H/HeJBir mice: Increased T helper cell type 1 response and ability to transfer disease. *J. Exp. Med.* **187,** 855–864, 1998.
38. Madsen, K. L., Doyle, J. S., Jewell, L. D., Tavernini, M. M., and Fedorak, R. N., *Lactobacillus* species prevents colitis in interleukin 10 gene-deficient mice. *Gastroenterology* **116,** 1107–1114, 1999.
39. Kullberg, M. C., Ward, M. J., Gorelick, P. L., Caspar, P., Hieny, S., Cheever, A., Jankovic, D., and Sher, A., *Helicobacter hepaticus* triggers colitis in specific-pathogen-free interleukin-10 (IL-10)-deficient mice through an IL-12-and gamma-interferon-dependent mechanism. *Infect. Immun.* **66,** 5157–5166, 1998.
40. Sutton, C. L., Kim, J., Yamane, A., Dalwadi, H., Wei, B., Landers, C., Targan, S. R., and Braun, J., Identification of a novel bacterial sequence associated with Crohn's disease. *Gastroenterology* **119,** 23–31, 2000.
41. Dalwadi, H. N., Wei, B., Kronenberg, M., Sutton, C. L., and Braun, J., The Crohn's disease-associated 12 bacterial antigen is the target of a CD4$^+$ T cell response in normal and colitic mice. *FASEB J.* **14,** A975, 2000.

Received November 9, 2001; accepted December 14, 2001